IAEA
International Atomic Energy Agency

INDC(KAS)-0002
Distr. NC

INDC International Nuclear Data Committee

Proceedings of the

Tenth AASPP Workshop on Asian Nuclear Reaction Database Development

Institute of Nuclear Physics, Almaty, Kazakhstan

24 – 27 June 2019

Edited by

Timur Zholdybayev
Institute of Nuclear Physics, Almaty, Kazakhstan

and

Naohiko Otuka
Nuclear Data Section, International Atomic Energy Agency, Vienna, Austria

September 2019

IAEA Nuclear Data Section, Vienna International Centre, A-1400 Vienna, Austria

Selected INDC documents may be downloaded in electronic form from
http://www-nds.iaea.org/publications/
or sent as an e-mail attachment.
Requests for hardcopy or e-mail transmittal should be directed to
nds.contact-point@iaea.org
or to:

Nuclear Data Section
International Atomic Energy Agency
Vienna International Centre
PO Box 100
A-1400 Vienna
Austria

Produced by the IAEA in Austria
September 2019

INDC (KAS)-0002
Distr. NC

Proceedings of the

Tenth AASPP Workshop on Asian Nuclear Reaction Database Development

Institute of Nuclear Physics, Almaty, Kazakhstan

24 – 27 June 2019

Edited by

Timur Zholdybayev
Institute of Nuclear Physics, Almaty, Kazakhstan

and

Naohiko Otuka
Nuclear Data Section, International Atomic Energy Agency, Vienna, Austria

September 2019

Abstract

The 10th Workshop on Asian Nuclear Reaction Database Development was held from 24-27 June 2019 at the Institute of Nuclear Physics in Almaty (Kazakhstan). This 10th workshop followed the workshops in Sapporo (Japan, 2010), Beijing (China, 2011), Pohang (Korea, 2012), Almaty (Kazakhstan, 2013), Mumbai (India, 2014), Sapporo (Japan, 2015), Beijing (China, 2016), Ulaanbaatar (Mongolia, 2017) and Gyeongju (Korea, 2018). The workshop was organized by Institute of Nuclear Physics in collaboration with the Asian Centres of the International Network of Nuclear Reaction Data Centres and supported by International Atomic Energy Agency. The topics of the workshop were sharing information on activities of the nuclear data centres, EXFOR compilation, data evaluation, computational simulations, software training and other related topics. The participants were attended from India, Japan, Kazakhstan, Uzbekistan, Mongolia, Turkey and the IAEA. In the workshop, 11 presentations were presented and summarized in these proceedings.

Table of Contents

Agenda

Date	Time	Topics	Speaker
June 24 (Mon)	**10:00~17:00**	EXFOR session	
	9.00~10.00	Forum Registration	
	10.00~17.00	Compilation	Responsible: Otsuka N.
	13.00~14.30	Lunch	
	19.00-21.00	Banquet	
June 25 (Tue)	**09:30~17:00**	EXFOR session	
	09.30~13.00	Compilation	Responsible: Otsuka N.
	13.00~14.30	Lunch	
	14.30~14.50	Uncertainties due to coincidence- summing correction in gamma ray spectroscopy	Otsuka N. (IAEA)
	14.50~15.10	Status of EXFOR activity in India and evaluation of neutron induced cross section	Devi Vidya (IET)
	15.10~15.30	Scattering problems of two-body systems	Odsuren M. (NUM)
	15.30~15.50	New data on the $^{12}C(p,\gamma)^{13}N$ yields	Ergashev F.Kh. (INP UZ)
	15.50~16.10	The structure of Ξ hypernuclei	Tada T. (Hokkido Univ.)
	16.00~18.00	POSTERS	
June 26 (Wed)	**9.30~13.00**		
	9.30~9.50	Investigation of elastic scattering and nucleon transfer in the interaction of deuterons with the $^{24-25}Mg$ nuclei	Artemov S.V. (INP UZ)
	9.50~10.10	Role of the dynamical polarization potential in explaining the low-energy data of alfa+^{12}C system	Kucuk Y. (Akdeniz Univ.)
	10.10~10.30	Interaction of 30 MeV energy protons with nuclei of mass A=27-209	Zholdybayev T.K. (INP KZ)
	10.30~10.50	Overview of EXFOR Compilation Activity in Mongolia between 2018 and 2019	Odsuren M. (NUM)
	10.50~11.20	Analyzing the (p,xp) and (p,xα) reactions on ^{59}Co at E=30 MeV by using the Statistical Models	Kucuk Y. (Akdeniz Univ.)
	11.20~11.40	Coffee-break	
	11.40~12.00	Experimental studies of cosmic rays at the laboratory of cosmic rays variations of Al-Farabi Kazakh National University	Mukhamejanov Y.S. (INP KZ)

	12.00~14.30	Lunch	
June 27 (Thu)	**9.30~15.00**		
	9.30~11.00	Plenary session	
	11.00~13.00	Summary of Forum results, closing of the Forum	
	13.00~15.00	Farewell Lunch	

Uncertainties due to Coincidence-Summing Correction in Gamma-Ray Spectrometry

N. Otuka[1], V. Semkova[2]

[1]*Nuclear Data Section, International Atomic Energy Agency, A-1400 Vienna, Austria*
[2]*Institute for Nuclear Research and Nuclear Energy, BG-1784, Sofia, Bulgaria*

Gamma-ray spectrometry with germanium detectors is a technique widely used in both basic and applied fields to identify and quantify the radioactive nuclides in samples. In the nuclear data field, it is routinely used in determination of activation cross sections. When the sample activity is weak, the counting statistics can be improved by increasing the volume of the detector or reducing the sample-detector distance. But it also increases the probability to detect several γ-rays in coincidence. Detectors cannot distinguish (1) energy deposition by two γ-rays carrying energies $E_{\gamma 1}$ and $E_{\gamma 2}$ from (2) energy deposition by a single γ-ray carrying $E_{\gamma}=E_{\gamma 1}+E_{\gamma 2}$. Due to this effect (coincidence-summing), the raw count overestimates or underestimates the real counts, and we have to correct the raw count for the effect (coincidence-summing correction). For example, this correction may become important when we use several γ-lines emitted from a single calibration source (*e.g.*, ^{152}Eu). This correction introduces additional uncertainty to the quantity of interest (*e.g.*, cross section), and it is important to develop a method to estimate the uncertainty in the coincidence-summing correction factor so that we can propagate it to the uncertainty in the quantity of interest (See [1-2] for uncertainty propagation in determination of activation cross sections.). There is not a common procedure to estimate the uncertainty in the coincidence-summing correction factor, and our attempt is briefly summarized in this report.

The model of correction factor calculation developed by Andreev et al. [3-4] and formulated with matrices by Semkov et al. [5] was adopted as the basis of our uncertainty propagation. In this formalism, the probability to detect a γ-ray for transition from level j to i without coincidence summing effect is expressed by

$$C_{0ji} = [\Sigma_p f_p (\delta_{pj} + x_{pj} + \Sigma_k x_{pk} x_{kj} + \Sigma_{k,l} x_{pk} x_{kl} x_{lj} + \ldots) a_{ji}$$

with

$$a_{ji} = [x_{ji} / (1+\alpha_{ji})] \varepsilon^p_{ji},,$$

where f_p is the probability of β transition from the precursor to level p, x_{ji} is the probability of γ transition or internal conversion, α_{ji} is the internal conversion coefficient, ε^p_{ji} is the peak efficiency, δ_{pj} is Kronecker's delta ($\delta_{pj}=1$ when $p=j$, otherwise $\delta_{pj}=0$). The transition probabilities are normalized such that their summation over the final states equal 1, namely $\Sigma_p f_p=1$ and $\Sigma_i x_{ji}=1$. Under the presence of the coincidence-summing effect, C_{0ji} is modified to

$$C_{1ji} = [\Sigma_p f_p (\delta_{pj} + b_{pj} + \Sigma_k b_{pk} b_{kj} + \Sigma_{k,l} b_{pk} b_{kl} b_{lj} + \ldots)$$

$$\times (a_{ji} + \Sigma_k a_{jk} a_{ki} + \Sigma_{k,l} a_{jk} a_{kl} a_{lj} + \ldots)$$

$$\times(\delta_{i0} + b_{i0} + \Sigma_k b_{ik} b_{k0} + \Sigma_{kl} b_{ik} b_{kl} b_{l0} + \ldots)$$

with

$$b_{kl} = x_{kl} - [x_{kl} / (1+\alpha_{kl})] \varepsilon^t_{kl},$$

where ε^t_{kl} is the total efficiency. If we define the coincidence-summing correction factor by

$$D_{ji} = C_{1ji} / C_{0ji},$$

its uncertainty can be propagated from the uncertainties in $\{f_p\}$, $\{x_{kl}\}$, $\{\alpha_{kl}\}$, $\{\varepsilon^p_{kl}\}$ and $\{\varepsilon^t_{kl}\}$. For example, the covariance of the β transition probability $\mathrm{cov}(f_p, f_{p'})$ is propagated to D_{ji} by

$$\Sigma_{pp'} (\partial D_{ji}/\partial f_p) \mathrm{cov}(f_p, f_{p'}) (\partial D_{ji}/\partial f_{p'}).$$

Table 1. Total and partial uncertainties in the coincidence-summing correction factor.

E_γ (MeV)	D_{ji}	Uncertainty in D_{ji} (%)					
		Total	f	x	α	ε^p	ε^t
242.7	1.17	0.92	0.00	0.13	0.00	0.00	0.91
326.6	1.23	1.04	0.00	0.35	0.00	0.00	0.98
475.4	1.16	0.92	0.00	0.17	0.00	0.00	0.90
563.2	1.18	0.88	0.00	0.08	0.00	0.00	0.88
569.3	1.17	0.92	0.00	0.13	0.00	0.00	0.91
604.7	1.10	0.56	0.01	0.00	0.00	0.00	0.56
795.9	1.10	0.70	0.00	0.08	0.00	0.00	0.70
802.0	1.16	0.91	0.00	0.17	0.00	0.00	0.90
1038.6	1.03	0.65	0.00	0.09	0.00	0.07	0.64
1168.0	0.92	0.54	0.00	0.05	0.00	0.19	0.50
1365.2	0.87	0.71	0.00	0.10	0.00	0.28	0.64

We applied our analytic formalism of the uncertainty propagation to γ-rays emitted following β decay of ^{134}Cs for a coaxial HPGe detector calibrated at EC-JRC IRMM. The detector was calibrated by using a set of monoenergetic standard sources and the peak and total efficiencies and their covariances for ^{134}Cs γ-lines were obtained through interpolation of the reference data with polynomial logarithmic function [6]. The nuclear data and their uncertainties were taken from data evaluated by DDEP [7].

Table 1 shows our preliminary estimation of the total and partial uncertainties in the correction factor. More detailed documentation of this work is under preparation [8].

References

[1] D.L. Smith, N. Otuka, Nucl. Data Sheets **113** (2012) 3006.
[2] N. Otuka, B. Lalremruata, M.U. Khandaker, A.R. Usman, L.R.M. Punte, Radiat. Phys. Chem. **149** (2018) 151.
[3] D.S. Andreev, K.I. Erokhina, V.S. Zvonov, I.Kh. Lemberg, Bull. A.S. USSR Phys. Ser. **37** No.8 (1973) 41.
[4] D.S. Andreev, K.I. Erokhina, V.S. Zvonov, I.Kh. Lemberg, Instrum. Exp. Tech. **15**, (1972) 1358.
[5] T.M. Semkow, G. Mehmood, P.P. Parekh, M. Virgil., Nucl. Instr. Meth. A**290**, 437 (1990).
[6] V. Semkova, Report GE/NP/03/2006/02/02, EC-JRC Institute for Reference Materials and Measurements (2006).
[7] M.-M. Bé, V. Chisté, C. Dulieu, X. Mougeot, V.P. Chechev, F.G. Kondev, A.L. Nichols, X. Huang, B. Wang, Table of Radionuclides Vol.7, Bureau International des Poids et Mesures, Sévres, 2013.
[8] V. Semkova, N. Otuka, A.J.M. Plompen, to be published in EPJ Web of Conf.

Status of EXFOR Activity in India and
Evaluation of Neutron Induced Cross Section

Vidya Devi

Institute of Engineering and Technology, Bhaddal, Ropar, Punjab, INDIA

Nuclear Data Physics Centre of India (NDPCI) is a research center for nuclear data activities in Bhabha Atomic Research Centre (BARC) in India. Bhabha Atomic Research Centre is the nodal centre for design, development and the application of nuclear technology for the welfare of mankind BARC, Mumbai, is part of DAE (Department of atomic Energy) and is the nodal centre for the collaboration with IAEA-NDS, CERN, NRDC and others. The BARC is responsible for theoretical, experimental nuclear physics research and code development for the implementation of Indian nuclear programme. This report summarizes the review of compilation status in India (**Appendix 1)**. In this report we will also briefly present some methods such as Unscented Transform technique and Monte Carlo method for the determination of the Uncertainty propagation. We generate and present the covariance information by taking into account various attributes influencing the uncertainties and also the correlations between them.

Data compilation GROUP in India

Vidya Devi (Gulshan Premi)	IET, Bhaddal, Ropar (Checker/Compiler)
B. Rudraswamy (Imran Pasha)	Bangalore University, Bangalore (compiler)
Ajay Tyagi (Aman Gandhi)	BHU, Varanasi (compiler)
Gayatri Mohanto	BARC, Mumbai (compiler, Numerical data collector)

Sandwich Formula:

The Sandwich formula for error propagation is first order sensitivity analysis method. Consider an independent variable vector x of order n, and dependent variable vector y of order m. Let $y = f(x)$, then the mean value of y is given as $\acute{y} \approx f(\acute{x})$ and the covariance matrix for Sandwich formula is [1-3]

$$C_y \approx H_x C_x H_X^T \quad C_y \approx H_x C_x H_X^T \tag{1}$$

Here C_x is $n \times n$ covariance matrix of x, C_y is $m \times m$ covariance matrix of y and H_x is the sensitivity matrix with elements $H_{xij} = \left(\frac{\partial f_i}{\partial x_j} \right) \left(i = 1,2,....,n \right)$.

This method works quite well for functions with small nonlinearity and small uncertainties.

Unscented Transform (UT) Method:

It is difficult to transform a probability density function (PDF) through a general nonlinear function that is why uncertainty propagation is also difficult. Unscented Transform method (UT) is based on two principles; it is easy to perform a nonlinear transformation on a single point, and, it is easy to find a set of individual points in state space whose sample PDF approximates the true PDF of a state vector [3]. Consider a primary variable vector x with mean $\acute{x}$ and covariance P. If we find a set of deterministic vectors called sigma points whose ensemble means and covariance are same as that of x. Then using these sigma points, on the known nonlinear functional relationship to obtain transformed vectors, we can calculate mean and covariance of transformed vectors.

Let X be $^{n\times 1}$ vector with mean $\overline{X}$ and covariance$P$. We choose $2n$ sigma points $X^{(i)}$ as follow:

$$X^{(i)}=\overline{X}+\overline{X}^{(i)},\quad i=1,2,\ldots,2n \quad X^{(i)}=\overline{X}+\overline{X}^{(i)},\quad i=1,2,\ldots,2n \tag{2}$$

where $\widetilde{X}^{(i)}=\left(\sqrt{nP}\right)_i^P$ and $\widetilde{X}^{(n+1)}=-\left(\sqrt{nP}\right)_i^T$, for $i=1,2,\ldots,n$. Here $\sqrt{nP}$ can be calculated using Cholesky factorization. Using these sigma points, we can calculate $2n$ transformed vectors (y). The mean and covariance are given by the formula

$$\overline{Y}=\sum_{i=1}^{2n}W^{(i)}Y^{(i)} \quad \overline{Y}=\sum_{i=1}^{2n}W^{(i)}Y^{(i)} \tag{3}$$

$$C=\sum_{i=1}^{2n}W^{(i)}\left(y^{(i)}-\overline{y}\right)\left(y^{(i)}-\overline{y}\right)^T \quad C=\sum_{i=1}^{2n}W^{(i)}\left(y^{(i)}-\overline{y}\right)\left(y^{(i)}-\overline{y}\right)^T \tag{4}$$

$W^{(i)}=1/2n,\quad i=1,2,\ldots,2n$ are weight coefficients.

Cross-Section:

$$\begin{aligned}\sigma_r&=\sigma_m Y\frac{C_r\lambda_r N_m\varepsilon_m I_m(1-e^{-\lambda_m t_{irrm}})e^{-\lambda_m t_{coolm}}(1-e^{-\lambda_m t_{coolm}})\alpha_m}{C_m\lambda_m N_r\varepsilon_r I_r(1-e^{-\lambda_r t_{irrr}})e^{-\lambda_r t_{coolr}}(1-e^{-\lambda_r t_{coolr}})\alpha_r}\\ \sigma_r&=\sigma_m Y\frac{C_r\lambda_r N_m\varepsilon_m I_m(1-e^{-\lambda_m t_{irrm}})e^{-\lambda_m t_{coolm}}(1-e^{-\lambda_m t_{coolm}})\alpha_m}{C_m\lambda_m N_r\varepsilon_r I_r(1-e^{-\lambda_r t_{irrr}})e^{-\lambda_r t_{coolr}}(1-e^{-\lambda_r t_{coolr}})\alpha_r}\end{aligned} \tag{5}$$

Here subscript *r* is for unknown reaction and subscript *m* is for monitor reaction. We define the vector *X* in similar way as discussed earlier to calculate the cross section using UT method.

Table 1. Interpolated detector efficiency using Sandwich Formula and UT method reaction and their corresponding covariance matrix Meghna et. al [4].

E_γ (keV)	Efficiency (ε_γ)	Correlation matrix
Sandwich Formula (Meghna et al.)		
84.2	0.062 ± 0.0040	1
743.3	0.023 ± 0.00028	0.15 1
UT Method		
84.2	0.0625 ± 0.0040	1
743.3	0.0234 ± 0.00028	0.145 1

Table 2. Measured neutron cross-section of ^{232}Th(n,2n)^{231}Th reaction and their corresponding covariance matrix Meghna et. al [4].

E_n (MeV)	σ (barn)	Correlation matrix
Sandwich formula (Meghna et al.)		
8.97 ± 0.34	1.82 ± 0.27	1
16.52 ± 0.30	0.62 ± 0.10	0.37 1
UT Method		
8.97 ± 0.34	1.833 ± 0.283	1
16.52 ± 0.30	0.627 ± 0.114	0.35 1

Table 3. Interpolated detector efficiency for ^{7}Li(p,n) reaction as neutron source using Sandwich Formula and UT method [5].

E_γ (MeV)	Efficiency (ε_γ)	Correlation matrix
Sandwich Formula (Meghna et al.)		
0.08421	2.15E-01 ± 2.36E-03	1
0.7433	3.37E-02 ± 3.62E-04	-4.20E-02 1
UT Method		
0.08421	2.15E-01 ± 2.37E-03	1
0.7433	3.37E-02 ± 3.61E-04	-4.05E-02 1

Table 4. Measurement of neutron cross section of $^{232}Th(n,2n)^{231}Th$ reaction at E_n = 10.49, 11.46, 18.36 and 15.03 MeV [5].

E_n (MeV)	σ (barn)	Correlation matrix		
Sandwich formula (Meghna et al.)				
10.49 ± 0.029	2.16 ± 0.31	1.00	.22	.19
14.46 ± 0.26	1.08 ± 0.13		1.00	.35
18.36 ± 0.24	0.45 ± 0.06			1.00
UT Method				
10.49 ± 0.029	2.18 ± 0.38	1.00	.21	.22
14.46 ± 0.26	1.08 ± 0.13		1.00	.39
18.36 ± 0.24	0.45 ± 0.05			1.00

Future Plan:

Participation in other NDPCI assigned work such as Journal survey, removing the duplication of entry.

Participation in the neutron and proton induced reaction cross-sections experiments to be held at BARC, Mumbai.

It will be of great interest to further examine the applications and performance of the UT method in complex reactor physics calculations and nuclear data evaluations.

References

[1] H. Kadvekar, A Preliminary Examination of the Application of Unscented Transformation Technique to Error Propagation in Nonlinear Cases of Nuclear Data Science, Nuclear Science and Engineering, **183** (2016).

[2] D. L. Smith, N. Otuka, Experimental Nuclear Reaction Data Uncertainties: Basic Concept and Documentation, Nuclear Data Sheets **113** (2012) 3006.

[3] D. Simon, Optimal State Estimation, John Wiley & sons, 2006.

[4] M. Karkera, H.Naik, S. Punchithaya, M.P.Karantha, S.S.Yeraguntla, S.V.Suryanarayana, S.Ganesan, V. Vansola, R. Makhwana, J. Rad. Nucl. Chem., **318** (2018) 1893.

[5] M. Karkera, S.S.Yeraguntla, S. Punchithaya, S.V.Suryanarayana, M.P.Karantha H.Naik, S.Ganesan, et al., Technical Report, DOI: 10.13140/RG.2.2.24664.34566 (2019).

Appendix 1: List of EXFOR Entries Compiled and Checked 2018-2019

S.No.	Entry No.	Reference	First Author
1.	G0512	J,JNR,314,1983,2017	H. Naik
2.	33106	J,ARI,127,92,2017	H. Naik
3.	33107	J,ARI,127,150,2017	R.Makwana
4.	33108	J,ARI,129,117,2017	H. Naik
5.	33109	J,EPJ/A,53,46,2017	P.Panikkath
6.	33110	J,JNR,314,457,2017	H. Naik
7.	33111	J,PR/C,96,024608,2017	S.Mukherjee
8.	33112	J,NSE,187,302,2017	M.S.Barough
10.	D6303	J,NP/A,960,53,2017	H.Kuma
11.	D6304	J,NP/A,964,86,2017	H. Naik
12.	D6305	J,PR/C,95,014614,2017	D.R.Chakrabarty
13.	D6306	J,PR/C,95,034615,2017	A.Kundu
14.	D6307	J,PR/C,95,064602,2017	A.Maiti
15.	D6308	J,PR/C,95,064603,2017	R.Pandey
16.	D6309	J,PR/C,96,014617,2017	A.Maiti
17.	D6310	J,PR/C,96,014620,2017	A.Sood
18.	D6311	J,PR/C,96,024603,2017	A.Pal
19.	D6312	J,PR/C,96,034620,2017	A.Shrivastava
20.	D6313	J,PR/C,96,044616,2017	S.K.Pandit
21.	D6314	J,PR/C,96,054613,2017	A.Parihari
22.	D6315	J,PR/C,96,064609,2017	A.Sen
23.	D6316	J,PR/C,95,014612,2017	S.Sodaye
24.	D6317	J,PR/C,95,024604,2017	R.Tripathi
25.	D6318	J,PR/C,95,034610,2017	E.Prasad
26.	D6319	J,PR/C,96,014614,2017	Khushboo
27.	D6320	J,PR/C,96,034613,2017	B.R.Behera
28.	D6321	J,PR/C,96,044607,2017	M.Nandy
29.	D6322	J,PR/C,96,044608,2017	R.Tripathi
30.	D6323	J,PR/C,96,044614,2017	A.Yadav
31.	D6324	J,PR/C,96,054605,2017	A.Kumar
32.	D6325	J,PR/C,96,054614,2017	V.R.Sharma
33.	G0513	J,RCA,106,345,2018	R.Ghosh
34.	D6327	J,EPJ/A,54,56,2018	S.Ali
35.	D6346	J,PR/C,98,034603,2018	M.Gull
36.	D6350	J,RCA,48,7,1989	R.Guin
37.	D6351	J,RCA,51,97,1990	R.Guin
38.	33118	J,RCA,37,63,1984	H.C.Jain
39.	33119	J,RCA,54,163,1991	A.Ramaswami
40.	33120	J,JRN,140,215,1990	A.G.C.Nair

Scattering Problems of Two-Body Systems

M. Odsuren[1], G. Khuukhenkhuu[1], A.T. Sarsembayeva[2], S. Davaa[1], B. Usukhbayar[1], A.Zolbayar[1], K. Kato[3]

[1]*School of Engineering and Applied Sciences and Nuclear Research Center, National University of Mongolia, Ulaanbaatar 210646, Mongolia*

[2]*School of Industrial Engineering after A. Burkitbaev, Satbayev University, Almaty, 0500013, Kazakhstan*

[3]*Nuclear Reaction Data Centre, Faculty of Science, Hokkaido University, Sapporo 060-0810, Japan*

Introduction

The complex scaling method (CSM) [1-4] and the orthogonal condition model (OCM) [5] have been successfully utilized in the description of resonance states in light nuclei. In this work, we apply the CSOCM [4, 6] to the ^{8}Be and investigate two-body resonances for α+α system. We calculate resonance energies in the complex energy plane applying the CSM to the relative motion between two α-clusters. From the viewpoint of a microscopic description of the relative motion between the α+α clusters it is important to take into account the Pauli exclusion principle in the inter-cluster motion of nucleons. The Gaussian and Harmonic Oscillator wave functions are applied. The calculation procedure of using the Pauli principle are different in these basis functions, however, the same results for two-body system are expected. Our calculated results of the resonance energy and decay width are satisfactorily in agreement with experimental data for the $J^{\pi}=0^{+}$, 2^{+} and 4^{+} states [7].

Complex Scaling Method

In the last quarter century, a remarkable development in the description of resonances in quantum many-body systems has been realized through application of the CSM.

Originally, the CSM was proposed by Aguilar, Combes, and Balslev in 1971 [1]. Simon advocated this method as a direct approach of obtaining many-body resonances. The use of "direct" implies that the resonance wave functions are directly obtained with complex energy eigenvalues of the quantum many-body system by solving an eigenvalue problem of the complex-scaled Schrodinger equation, $H^{\theta}\Psi^{\theta} = E^{\theta}\Psi^{\theta}$ with a real scaling angle θ. In the CSM, we take the imaginary value $i\theta$as a parameter of the transformation.

The CSM has been proposed to solve the resonance states in the similar way as bound state problems. In the CSM, the distance of the relative coordinate is rotated as

$r \longrightarrow re^{i\theta}$ in the complex coordinate plane by introducing a real parameter θ. Therefore, the Schrödinger equation

$$\hat{H}\Psi\rangle = E\Psi\rangle \tag{1}$$

is rewritten as

$$\hat{H}(\theta)\Psi^{\theta}\rangle = E^{\theta}\Psi^{\theta}\rangle \tag{2}$$

where $\hat{H}(\theta)$ and Ψ^{θ} are the complex scaled Hamiltonian and the wave function, respectively. $U(\theta)$ operates on a function Ψ, that is,

$$\Psi^{\theta} = U(\theta)\Psi(r) = e^{\frac{3}{2}i\theta}\Psi\left(re^{i\theta}\right). \tag{3}$$

The eigenvalues and eigenstates are obtained by solving the complex scaled Schrodinger equation Eq. (2). The eigenvalues of resonance states are found as $E^{\theta} = E_r - i\,\Gamma_r/2$, where E_r is resonance energy and Γ_r-width of the resonant state. More detailed explanation of the CSM is given in Refs. [1,2]. The complex scaled Hamiltonian of inter cluster motion is given by

$$\hat{H}(\theta) = U(\theta)\hat{H}U^{-1}(\theta). \tag{4}$$

Two body interaction

For the alpha-alpha system the Hamiltonian is expressed as

$$\hat{H} = \sum_{i=1}^{2}\hat{T}_i - \hat{T}_{c.m.} + V_{\alpha\alpha}^{Nucl}(r) + V_{\alpha\alpha}^{Coul}(r). \tag{5}$$

As mentioned at the beginning, in this work we use two different basis sets as follows: (i) A Gaussian basis for the radial part is given as

$$\phi_l^i(r) = N_l^i r^l exp\left(\frac{-1}{2b_i^2}r^2\right)Y_{lm}(r). \tag{6}$$

Here $i = 0,1,2,\ldots$, and N_l^i is normalization constants expressed as $N_l^i = \frac{1}{b_i^{l+3/2}}\left\{\frac{2^{l+2}}{(2l+1)!!\sqrt{\pi}}\right\}^{1/2}$ and b_i is the size parameter of Gaussian function described as $b_i = b_0\gamma^{i-1}$. Where b_0 and γ are the first term and a common ratio in the geometric progression, respectively.

(ii) Harmonic oscillator wave function for radial part is

$$\phi_{nl}(r) = N_l^n\left(\frac{r}{b_F}\right)^l L_n^{l+\frac{1}{2}}\left(\left(\frac{r}{b_F}\right)^2\right)exp\left(\frac{-1}{2b_F^2}r^2\right)Y_{lm}(r). \tag{7}$$

Here $L_n^{l+1/2}$ are Laguerre polynomials for the angular momentum l and N_l^n denotes the normalization constants as given by $N_l^n = \left\{\frac{2\Gamma(n+1)}{b_F^3\Gamma\left(l+n+\frac{3}{2}\right)}\right\}^{1/2}$. The size parameter of relative motion of two alpha-cluster b_F is taken as 0.967 fm which corresponds to a single particle size parameter $b_0 = 1.3975$ fm employed to fit the observed r.m.s. radius of ^{4}He. In the case (i), we introduce the Pauli-potential $V_{\alpha\alpha}^{P}(r) = \lambda|\chi_F\rangle\langle\chi_F|$, where the strength λ is chosen as 10^7 MeV, which is enough to push up the Pauli-forbidden states into the unphysical energy region.

Results and Discussion

In the numerical calculation, we have used two different basis set: (i) Gaussian basis function, and (ii) harmonic oscillator wave function. In Eq. (5), the Buck [8] and folding [9] potentials are applied for the Gaussian basis function, but also the folding potential is employed in the harmonic oscillator wave function. According to the Buck-potential, the Pauli-forbidden states need not involve on the alpha-alpha system because of the Pauli principle effect is estimated by an appropriate choice of alpha-alpha potential. However, it is important to take into account of the forbidden states when we use the folding potential of the effective nuclear interaction.

From Eq. (2) the eigenvalues are obtained distributions of which on the complex energy plane are shown **Fig. 1.**

Fig. 1 shows the complex energy eigenvalues of 2^+ state which is obtained by Buck potential for Gaussian basis at different θ on the complex energy plane. The resonance energy solution must be stationary for changing the values of θ as explained in Ref. [6].

We can see that for different θ segregated energy points are observed, but also these are almost unchanged the position by various θ on the complex energy plane (see **Fig. 1**). **Fig. 1** shows that there is significant energy point segregation around the location resonance state at the complex scaled plane.

θ - and b-trajectories are displayedin **Fig. 2**. We chose the steps of b-trajectories by $b = b_0 + 0.1\kappa$ here $\kappa = 1,2 \ldots ,10$ which were calculated by two methods: changing parameter b and θ is fixed for each b-trajectories, and by the same b for every θ-trajectories, here θ is changing parameter and taken by $\theta = \theta_0 + \kappa$ where $\kappa = 0,2,4 \ldots ,20$.

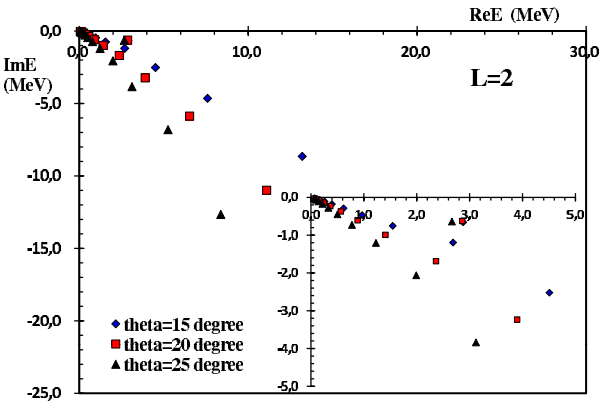

Fig. 1. The resonance eigenvalues at $J^{\pi}=2^{+}$ for the different θ. Here Buck-potential is used for Gaussian basis.

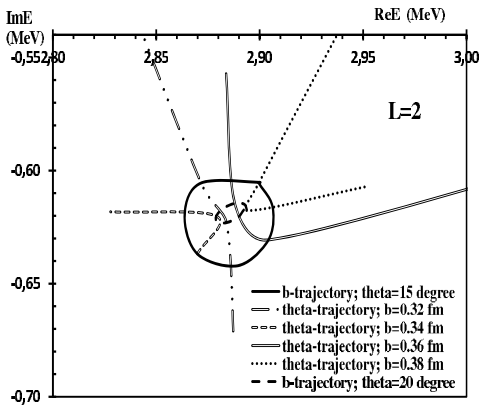

Fig. 2. The θ and b-trajectory at $J^{\pi}=2^{+}$. The Buck-potential and Gaussian basis are used.

It can be seen from **Fig. 2**, the resonance states are accurately described when the behavior of the θ - and b-trajectories are created well. The calculated result of harmonic oscillator wave function for folding potential is displayed in **Fig. 3**.

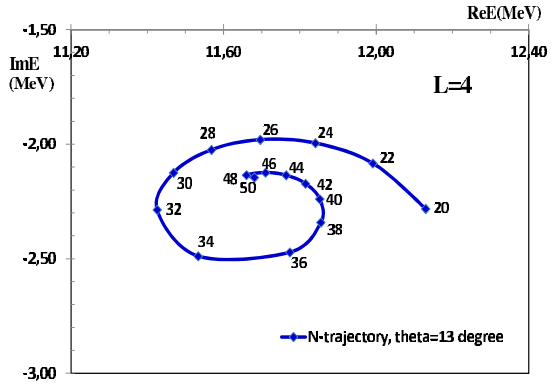

Fig. 3. The N-trajectory at $J^{\pi}=4^{+}$. The folding potential and harmonic oscillator wave function are used.

Fig. 3 shows the N-trajectories at $\theta = 13$ and $N = N_0 + k$ here $k = 0,2,4,\ldots,30$. The accurate values of resonances are taken into account by θ- and N-trajectories for harmonic oscillator wave function. The spiral curve represents the N-trajectory followed by the basis states when its size increases. The approach of the energy point is round $N = 46 - 50$.

In this work we have presented different methods to calculate resonance state in the two-body system by CSOCM. The θ-, b- and N-trajectories are performed in order to determine the resonance states for different method.

References

[1] Y.K. Ho, Phys. Rep. **99** (1983) 1.
[2] T. Myo, Y. Kikuchi, H. Masui, K. Katō, Prog. Part. Nucl.Phys. **79** (2014) 1.
[3] M. Odsuren, K. Kato, M. Aikawa, T. Myo, Phys. Rev. **C89** (2014) 034322.
[4] M. Odsuren, K. Kato, M. Aikawa, Nucl. Data Sheets **120** (2014) 126.
[5] S. Saito, Prog. Theor. Phys.**40** (1968) 893; **41** (1969) 705; Prog. Theor. Phys. Suppl. **62** (1977) 11.
[6] A. T. Kruppa, K. Katō, Prog. Theor. Phys. **84** (1990) 1145.
[7] F. Ajzenberg-Selove, Nucl. Phys. **A490**(1988) 1.
[8] B. Buck, H. Friedrich, C. Wheatley, Nucl. Phys, **A275**(1977) 246.
[9] E. W. Schmid, K. Wildermuth, Nucl. Phys. **26**(1961) 463.

New Data on the $^{12}C(p,\gamma)^{13}N$ Yields for the EXFOR Library

F.Kh. Ergashev[1], S.V. Artemov[1], A.A. Karakhodzhaev[1], O.R. Tojiboev[1], N. Burtebayev[2], Sh.Kh. Eshkobilov[3], N. Otuka[4]

[1]*Institute of Nuclear Physics, Tashkent, Uzbekistan*
[2]*Institute of Nuclear Physics, Almaty, Kazakhstan*
[3]*Research Institute of Physics of Semiconductors and Microelectronics at the National University of Uzbekistan*
[4]*Nuclear Data Section, International Atomic Energy Agency, A-1400 Vienna, Austria*

1. Introduction

The EXFOR library has become the most comprehensive compilation of experimental nuclear reaction data. It contains cross sections and other nuclear reaction quantities induced by neutron, charged-particle and photon beams. Compilation is mandatory for all low and intermediate energy (≤ 1 GeV) neutron and light charged-particle ($A \leq 12$) induced reaction data. Heavy-ion ($A \geq 13$) and photon induced reaction data are also compiled on a voluntary basis [1].

But experimental data for several nuclear reactions are not much enough in the EXFOR library due to lack of their measurements. The capture yield of the astrophysically important proton radiative capture reaction $^{12}C(p,\gamma)^{13}N$ at the energy below 300 keV is such an example. If we look for the capture yield data of this reaction by specifying "Quantity" type as PY (product yield) or TT* (thick target yield) at the IAEA NDS EXFOR web retrieval site, we find only three relevant articles [2-4]. The result of the search (**Fig. 1**) shows that these experimental works covers the proto energy above 350 keV. Since the capture yield drastically decreases as the energy decreases, it is desirable to have more data points at the lower energy from the view of astrophysical application. This article discusses EXFOR compilation of our new experimental results covering an extremely low energy region down to 190 keV, which published in the journals Nuclear Instruments and Methods in Physics Research in 2016 [5] and International Journal of Modern Physics in 2019 [6].

2. Experimental method

The activation method is advantageous at measuring very low cross sections because it allows the geometry of measurements close to 4π. Using this method with a pair of the NaI scintillators, one can detect β-particles, γ-quanta or γγ-coincidences due to pair annihilation (in the case of β^+-radioactive residual nucleus) in the event counting mode with large detection efficiency instead of applying the precise gamma-ray spectrometry with a germanium detector having smaller efficiency. It automatically provides the cross section or yield of the reaction, and the result does not depend on

details of the γ-ray decay scheme (as long as the decay data such as decay emission probabilities are well established) and γ-ray angular distributions.

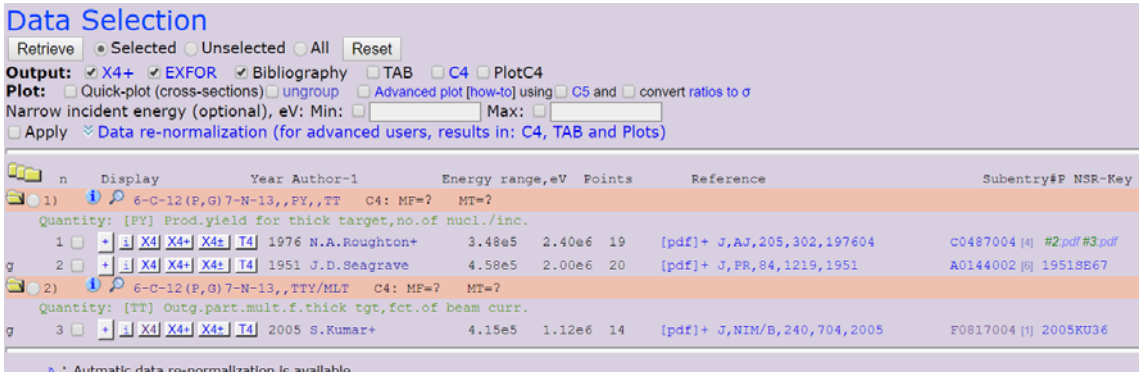

Fig. 1. Result of search for experimental data from the library EXFOR for the reaction $^{12}C(p,\gamma)^{13}N$ with quantity product yields and thick target yields (PY; TT*)

A variant of the activation method was previously developed and assembled on the ion guide of the electrostatic accelerator EG-2 of the Physics Faculty of the National University of Uzbekistan (NUUz) [5]. The accelerator is located at 6 meters underground to reduce the background of cosmic radiation. It covers the energy range of approximately 150–1500 keV with the $^{1}H^{+}$ ions external beam intensity of about 20 μA and the energy spread of ~ 2.5 keV (FWHM) [7].

The $^{12}C(p,\gamma)^{13}N$ capture yields for a carbon target thicker than the stopping length (range) were measured for the first time by using this method at the energies 190, 200 and 210 keV in addition to our previously obtained data within the interval 230-650 keV [5-6].

3. Results

The obtained data are presented in the **Fig. 2** together with the existing literature data. The curve is our analytical approximation of the yield energy dependence found in [5].

Table 1 presents the results of the measurements of proton radiative capture reaction $^{12}C(p,\gamma)^{13}N$ yields at the extremely low energy region newly reported in Ref. [6]. The capture yield data published in Refs. [5-6] were compiled by us for EXFOR D0953 (see Appendix).

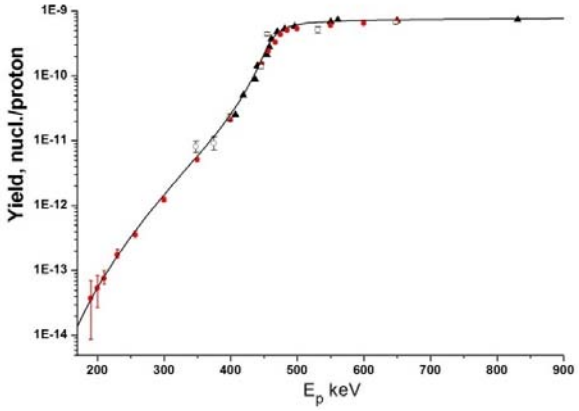

Fig. 2. Energy dependence of the capture yield (number of capture events per incident proton) for the reaction $^{12}C(p,\gamma)^{13}N$. Black triangles and open circles are the data from [3], [4], respectively.

Table 1. The yields $Y(E)$ of the reaction $^{12}C(p,\gamma)^{13}N$

N	E_p, keV	$Y(E)$, captures/proton [6]
1	190	$3.96 \cdot 10^{-14} \pm 3.09 \cdot 10^{-14}$
2	200	$5.62 \cdot 10^{-14} \pm 2.89 \cdot 10^{-14}$
3	210	$8.06 \cdot 10^{-14} \pm 1.87 \cdot 10^{-14}$

References

[1] N. Otuka et al. Nucl. Data Sheets **120** (2014) p.272.
[2] J.D. Seagrave, Phys. Rev. **84** (1951) 1219 (EXFOR A0144.002).
[3] N.A. Roughton, M.J. Fritts, R.J. Peterson, C.S. Zaidins, C.J. Hansen, Astrophys. J. **205** (1976) 302 (EXFOR C0487.004).
[4] S.Kumar, S.V.Kumar, G.L.N.Reddy, V.Kain, J.V.Ramana, V.S.Raju et al., Nucl. Instrum. Meth. Phys. Res. B**240** (2005) 704 (EXFOR F0817.004).
[5] S.V. Artemov et al. Nucl. Instr. Meth. Phys. Res. A**825** (2016) 17
[6] S.V.Artemov et al. Int. J. Mod. Phys.: Conf. Ser. **49** (2019) 1960013
[7] M.K. Aliev, G.R. Alimov, Sh.S. Baratbayev, et al., Uzb. J. Phys. **10** (2008) (№6) 410

Appendix: EXFOR Entry D0953 compiling $^{12}C(p,\gamma)^{13}N$ capture yields published in Refs.[5-6]

```
ENTRY            D0953   20190801                                D095300000001
SUBENT        D0953001   20190801                                D095300100001
BIB                 10         23                               D095300100002
TITLE      A modified activation method for reaction total cross  D095300100003
            section and yield measurements at low astrophysically D095300100004
            relevant energies                                     D095300100005
AUTHOR     (S.V.Artemov, S.B.Igamov, A.A.Karakhodjaev, G.A.Radyuk,D095300100006
            O.R.Tojiboyev, U.S.Salikhbaev, F.Kh.Ergashev, I.V.Nam,D095300100007
            M.K.Aliev, I.Kholbaev, R.F.Rumi, R.I.Khalikov,        D095300100008
            Sh.Kh.Eshkobilov, T.M.Muminov)                        D095300100009
INSTITUTE  (4UZ UZB,4UZ NUU)                                      D095300100010
REFERENCE  (J,NIM/A,825,17,2016)                                  D095300100011
           (J,IMP/CS,49,1960013,2019) 3 new points at 190-230 keV D095300100012
FACILITY   (ACCEL,4UZ NUU) EG-2 "SOKOL"                           D095300100013
METHOD     (ACTIV,BCINT)                                          D095300100014
           (COINC) gamma-gamma coincidence                        D095300100015
DETECTOR   (NAICR,NAICR)                                          D095300100016
            for annihilation gamma detection, 160 mm x 100 mm     D095300100017
            surrounded by Pb shield (50 mm thick)                 D095300100018
DECAY-DATA (7-N-13,9.965MIN,DG,511.,2.)                           D095300100019
ERR-ANALYS (DATA-ERR) Uncertainty due to                          D095300100020
            - Counting statistics;                                D095300100021
            - Beam current integration;                           D095300100022
            - gamma-gamma coincidence detection efficiency;       D095300100023
            - Beam energy determination.                          D095300100024
HISTORY    (20190723C) Feruzjon Ergashev                          D095300100025
ENDBIB              23          0                                 D095300100026
COMMON               1          3                                 D095300100027
EN-RSL-FW                                                         D095300100028
KEV                                                               D095300100029
 2.5                                                              D095300100030
ENDCOMMON            3          0                                 D095300100031
ENDSUBENT           30          0                                 D095300199999
SUBENT        D0953002   20190801                                D095300200001
BIB                  2          2                                 D095300200002
REACTION   (6-C-12(P,G)7-N-13,,PY,,TT)                            D095300200003
STATUS     (TABLE) Plotted in Fig.7, Nucl.Instr.Meth.A825(2016)17 D095300200004
ENDBIB               2          0                                 D095300200005
NOCOMMON             0          0                                 D095300200006
DATA                 3         14                                 D095300200007
EN         DATA       DATA-ERR                                    D095300200008
KEV        PRD/INC    PRD/INC                                     D095300200009
 230.         1.85E-13   2.82E-14                                  D095300200010
 257.         3.71E-13   3.47E-14                                  D095300200011
 300.         1.29E-12   6.90E-14                                  D095300200012
 350.         5.38E-12   1.48E-13                                  D095300200013
 400.         2.26E-11   5.75E-13                                  D095300200014
 447.         1.62E-10   1.62E-12                                  D095300200015
 457.         2.57E-10   4.62E-12                                  D095300200016
 467.         3.50E-10   1.45E-12                                  D095300200017
 475.         4.57E-10   8.68E-12                                  D095300200018
 485.         5.32E-10   1.01E-11                                  D095300200019
 500.         5.67E-10   1.13E-11                                  D095300200020
 550.         6.37E-10   1.07E-11                                  D095300200021
 600.         6.77E-10   1.26E-11                                  D095300200022
 650.         7.26E-10   1.20E-11                                  D095300200023
ENDDATA             16          0                                 D095300200024
ENDSUBENT           23          0                                 D095300299999
SUBENT        D0953003   20190801                                D095300300001
BIB                  2          3                                 D095300300002
REACTION   (6-C-12(P,G)7-N-13,,PY,,TT)                            D095300300003
STATUS     (TABLE) Plotted in Fig.1 of Int.Mod.Phys.Conf.Ser.     D095300300004
           49(2019)1960013,2019                                   D095300300005
ENDBIB               3          0                                 D095300300006
NOCOMMON             0          0                                 D095300300007
```

```
DATA                3          3                                  D095300300008
EN          DATA       DATA-ERR                                   D095300300009
KEV         PRD/INC    PRD/INC                                    D095300300010
 190.          3.96E-14   3.09E-14                                D095300300011
 200.          5.62E-14   2.89E-14                                D095300300012
 210.          8.06E-14   1.87E-14                                D095300300013
ENDDATA              5          0                                  D095300300014
ENDSUBENT           13          0                                  D095300399999
ENDENTRY             3          0                                  D095399999999
```

The Structure of Ξ Hypernuclei

T. Tada[1], M. Kimura[1], M. Isaka[2]

[1]*Department of Physics, Hokkaido University, 060-0810 Sapporo, Japan*
[2]*Hosei University, 102-8160 Tokyo, Japan*

The basic motivation of hypernuclei physics is the investigation of baryon-baryon interactions. Investigation of baryon-baryon interactions means generalization from nucleon-nucleon interaction to baryon-baryon interaction. Hyperon-nucleon interactions related to the equation of state (EoS) of the neutron star. If we consider the mixing of hyperon, the EoS would be soften. Then the EoS cannot reproduce the maximum mass $2.0M_{\odot}$[1,2]. This problem is known as the "hyperon puzzle." The hyperon puzzle can be solved if strong repulsions exist not only in *NNN* channels but also in *YNN* and *YYN* channels [3].

Baryon-baryon interaction in $S=-1$ sector has been investigated especially for Λ*N* interaction by experimental and theoretical work [4, 5]. For Λ hypernuclei, there is a systematic calculation of a single Λ binding energy B_{Λ} by using an extended version of antisymmetrized-molecular-dynamics (AMD) in the mass regions from *A*=9 up to *A*=51[6]. It reproduced experimental data of B_{Λ}.

The next challenge is the investigation of baryon-baryon interaction in $S=-2$ sector. But there are only a few numbers of the observation for Ξ hypernuclei by emulsion. The production experiment of ${}^{12}\mathrm{C}(K^-,K^+){}^{12}_{\Xi}\mathrm{Be}$ will be performed at Japanese facility of the Japan Proton Accelerator Research Complex(J-PARC). Then we calculated the energy gain of ${}^{12}_{\Xi}\mathrm{Be}$ hypernuclei by using an extended version of AMD.

In AMD, the Ξ hypernuclei wave function consists of *A* nucleons and a Ξ particle which is described by the parity-projected wave function,

$$\Psi^{\pi}=\hat{P}^{\pi}\Psi_{int}, \tag{1}$$

$$\Psi_{\mathrm{int}}=\varphi_{\Xi}\otimes\Psi_{N},\qquad \Psi_{N}=\frac{1}{\sqrt{A!}}\det\{\psi_i(\boldsymbol{r}_j)\}, \tag{2}$$

$$\psi_i(\boldsymbol{r}_j)=\phi_i(\boldsymbol{r}_j)\cdot\chi_i\cdot\eta_i, \tag{3}$$

$\hat{P}^{\pi}$ is the parity projector and Ψ_{int} is intrinsic wave function,

$$\phi_i(\boldsymbol{r})=\sum_{\sigma=x,y,z}\left(\frac{2\nu_{\sigma}}{\pi}\right)^{\frac{1}{4}}exp(-\nu_{\sigma}(r-Z_i)_{\sigma}^2), \tag{4}$$

$$\chi_i = \alpha_i \chi_\uparrow + \beta_i \chi_\downarrow, \tag{5}$$

$$\eta_i = proton\ or\ neutron, \tag{6}$$

$$\varphi_\Xi(\boldsymbol{r}) = \sum_{m=1}^{M} c_m \varphi_m(\boldsymbol{r}), \qquad \varphi_m(\boldsymbol{r}) = \phi_m(\boldsymbol{r}) \cdot \chi_m \cdot \eta_m, \tag{7}$$

$$\phi_m(\boldsymbol{r}) = \sum_{\sigma=x,y,z} \left(\frac{2\nu_\sigma}{\pi}\right)^{\frac{1}{4}} exp(-\nu_\sigma (r - z_m)_\sigma^2), \tag{8}$$

$$\chi_m = \alpha_m \chi_\uparrow + \beta_m \chi_\downarrow, \tag{9}$$

$$\eta_m = \Xi^- \ or\ \Xi^0, \tag{10}$$

where ψ_i is the *i*th nucleon single-particle wave packet consisting of spatial ϕ_i, spin χ_i, and isospin η_i parts. The variational parameter are the centroids of Gaussian Z_i and z_m, width parameters ν_σ, spin directions $\alpha_i, \beta_i, \alpha_m$ and β_m and coefficients c_m.

The Hamiltonian in this work is given as

$$\hat{H} = \hat{T}_N + \hat{V}_{NN} + \hat{T}_\Xi + \hat{V}_{\Xi N} + \hat{V}_{Coul}, \tag{11}$$

$\hat{T}_N$ and $\hat{T}_\Xi$are the kinetic energy of the nucleons and the kinetic energy of Ξ particle. $\hat{V}_{NN}$ and $\hat{V}_{\Xi N}$ are an effective nucleon-nucleon interaction and an effective ΞN interaction. We used Gogny D1S interaction [7] and *YN G*-matrix interaction derived from the Nijmegen potential named ESC08c [8, 9]. The *YNG* interaction depends on the Fermi momentum k_F. In this work we apply $k_F = 1.07 fm^{-1}$. $\hat{V}_{Coul}$ is proton-proton and proton-Ξ^- Coulomb interaction which is approximated by the sum of seven Gaussians. We have performed variational calculation for ${}^{12}_{\Xi}$Be. We ignored the $\Xi^0 + {}^{11}$Be channel because the $\Xi^- + {}^{11}$B channel is dominant [10].

Fig. 1. Shows the energy gain of ${}^{12}_{\Xi}$Be. The binding energy of Ξ is defined as the difference in energy between the ground state of the core nucleus and the hypernuclei states,

$$B_{\Xi} = B\left({}^{A+1}_{\Xi}X\right) - B\left({}^{A}X_{g.s.}\right). \tag{12}$$

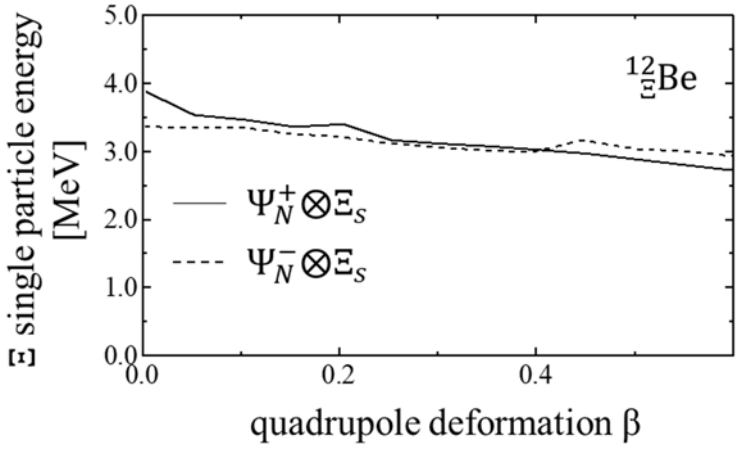

Fig. 1. The single-particle energies of Ξ_s of $^{12}_{\Xi}$Be as a function of quadrupole deformation of the core nucleus ^{11}B. The solid (dashed) line shows the energy of Ξ_s coupled to the positive (negative) parity state of ^{11}B.

In the future, we will calculate the level structure of $^{12}_{\Xi}$Be and compare with the experimental data in order to get the information of Ξ*N* interaction.

References

[1] P. B. Demorest, T. Pennucci, S. M. Ransom, M. S. E. Roberts, and J. W. Hessels, Nature (London) **467** (2010) 1081.
[2] J. Antoniadis et al., Science **340** (2013) 1233232.
[3] S. Nishizaki, Y. Yamamoto, and T. Takatsuka, Prog. Theor. Phys. **105** (2001) 607; **108** (2002) 703.
[4] D. J. Millener, Nucl. Phys. **A804** (2008) 84.
[5] E. Hiyama and T. Yamada, Prog. Part. Nucl. Phys. **63** (2009) 339, and references therein.
[6] M. Isaka, Y. Yamamoto and Th. A. Rijken, Phys. Rev. **C94** (2016) 044310.
[7] J. Decharg´e and D. Gogny, Phys. Rev. **C21** (1980) 1568.
[8] T. Rijken, M. Nagels, and Y. Yamamoto, Prog. Theor. Phys. Suppl. **185** (2010) 14.
[9] M. N. T. Rijken and Y. Yamamoto, Genshikaku Kenkyu **57** (2013) 6.
[10] H. Matsumiya et al., Phys. Rev. **C83** (2011) 024312.

Investigation of Elastic Scattering and Nucleon Transfer in the Interaction of Deuterons with the $^{24\text{-}25}$Mg Nuclei

S.V. Artemov[1], N. Burtebayev[2], F.Kh. Ergashev[1], A.A. Karakhodzhaev[1], O.R. Tojiboev[1]

[1] *Institute of Nuclear Physics, Tashkent, Uzbekistan*
[2] *Institute of Nuclear Physics, Almaty, Kazakhstan*

Introduction

The nucleon transfer between the magnesium and aluminum isotopes was studied in the works [1-5]. At that, the asymptotical normalization constants (ANC) for the {^{24}Mg+p/n} single particle configurations were determined only in the works of S.V. Artemov, S.B. Igamov et al. (see [6] and references therein). These value are important for estimation of the astrophysical S-factor for radiative capture of the proton by the ^{24}Mg nucleus, which is the first link in the Mg-Al chain ^{24}Mg(p,γ)^{25}Al (β^+)^{25}Mg(p,γ)^{26}Al(β^+)^{26}Mg. The mechanism of formation of ^{26}Mg isotope has become the key for confirming the stellar nucleosynthesis models. Therefore, it is necessary to define more exactly the ANC values of the proton-bound states {^{24}Mg+p}.

This paper presents the results of the analysis in the framework of the modified distorted wave method (MDWBA) [7] the reactions of a nucleon transfer ^{24}Mg(d,p)^{25}Mg, ^{25}Mg(d,t)^{24}Mg and ^{24}Mg(d,n)^{25}Al involving the suitable literature data and measured by us differential cross sections (DCS) of the reactions ^{25}Mg(d,t)^{24}Mg and ^{24}Mg(d,p)^{25}Mg to specify the ANC values of the single-particle configurations ^{24}Mg+n→^{25}Mg and ^{24}Mg+p→^{25}Al. The spectroscopic factor for ^{25}Mg$_{g.s.}$ as ^{24}Mg+n was defined by the comparative analysis of the reactions ^{25}Mg(d,t)^{24}Mg and ^{24}Mg(d,p)^{25}Mg.

Experimental setup

The experimental setup was earlier developed and mounted on the ion line of the accelerator U-150M (INP RKaz) in collaboration of the INP RUz and INP RKas scientists [8]. The measurement technique includes specialized reaction chamber, target and detecting systems, spectrometric electronics, which implements the ΔE-E-method, and specially developed software for data acquisition and processing. The highly enriched metallic foils of ^{24}Mg and ^{25}Mg with thicknesses of 0.82 and 0.78 mg/cm^2 were used as magnesium targets.

The DCS for deuteron scattering on ^{24}Mg and ^{25}Mg nuclei at E_d=14.5 MeV and 18.0 MeV as well as the reaction ^{24}Mg(d,p)^{25}Mg were measured for the neutron stripping process to the states E*=0.0 MeV, 5/2+; 0.585 MeV, ½+; 0.975 MeV, 3/2+, 1.61 MeV, 7/2+; 1.96 MeV, 5/2+ and 2.56 MeV, 1/2+ at E_d=14.5 MeV. Also the DCs of

the reaction ^{25}Mg(d,p)^{26}Mg were measured for the neutron stripping to the states E*=0.0 MeV, 0+; 1.81 MeV, 2+; 2.938 MeV and the DCS of the reaction ^{25}Mg(d,t)^{24}Mg were measured for population of the E*=0.0 MeV, 0+; and 1.37 MeV, 2+ states.

The systematic errors in the measured cross sections are mainly associated with the uncertainty of the target thickness (~5%), the solid angle of the spectrometer (1%). The statistical errors was 1-5% in the main maximum of the angular distributions, and so the total experimental errors as a rule did not exceed 7-10%.

Experimental data and MDWBA analysis

For the peripheral nucleon transfer reaction $A(x,y)B$, $x=y+N$ and $B=A+N$ the DCS is presented in the form:

$$\sigma(E,\theta) = \sum_{j_B j_x} C^2_{AN} C^2_{yN} R_{l_B j_B l_x j_x}(E,\theta) \tag{1}$$

$$R_{l_B j_B l_x j_x}(E,\theta) = \frac{\sigma^{DW}_{l_B j_B l_x j_x}(E,\theta)}{b^2_{AN} b^2_{YN}} \tag{2}$$

Here C^2_{AN} and C^2_{yN} are the squared ANCs of overlap integrals at two relevant nucleon bound states, ($A+N$) and ($y+N$). The values b and σ^{DW}, which is calculated using the DWUCK5 code, depend on geometry parameters r_0, a of the Woods-Saxon (W-S) potential.

As it is shown in MDWBA, for the peripheral transferring process a function $R(E,\theta)$ is insensitive to ambiguities of the geometry parameters of the bound state potential. So that is a test –is the reaction peripheral.

The optical model parameters (OP) needed for calculation of the distorted wave functions in the entrance and exit channels of the reactions were taken either from the articles containing the analyzed experimental data or global OP. At deuteron energies corresponding to our experiments the OP were checked by description of our elastic scattering data. It was found that the global OP from [9, 10] fits our data rather well (see **Fig. 1**). For triton channel the OP parameters from [11] and for proton channels from [12] were used.

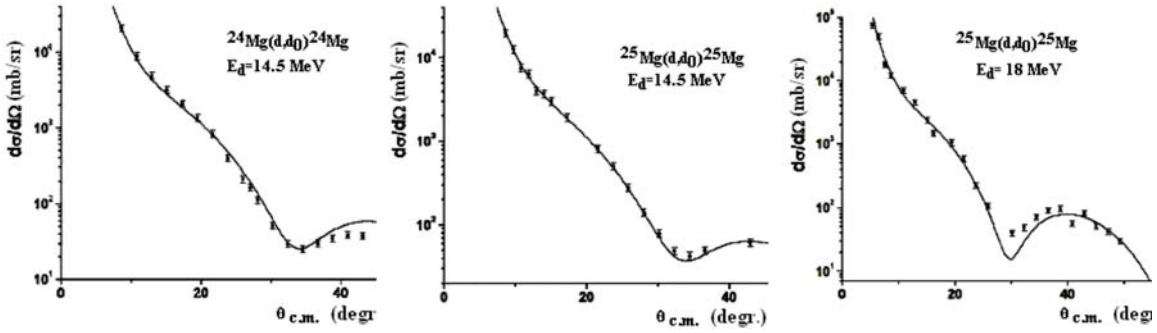

Fig. 1. DCS of the elastic scattering of deuterons on magnesium isotopes. Curves are the optical model fitting.

For obtaining the ANC ^{25}Mg→^{24}Mg+n by the MDWBA analysis the DCSs of the reaction ^{25}Mg(d,t)^{24}Mg at 14.8 MeV were taken from [13], at 18 MeV [14], at 15.3 and 18.0 MeV from [15] as well as our last data at 14.5 MeV [6]. The value of ANC $C^2_{d\to p+n}$ =0.774 fm^{-1} [16] has been used here and later. To verify the validity of MDWBA application, the corresponding $R(b)$ functions were previously investigated. In **Fig. 2** the result of DWBA calculations with different sets of the optical parameters and the experimental DCSs of the reaction ^{25}Mg(d,t)^{24}Mg measured by us are presented. The behavior of $R(b)$ at the energy E$_d$=14.5 MeV is illustrated in the insertion of the left picture, where all values are given in the arbitrary units. One can see that the value of R is very weakly dependent on the change of argument b at variation of geometric parameters of the bound state W-S potential (1.0 fm≤r_0≤1.4 fm, 0.4 fm≤a≤0.8 fm). It should be mentioned that behavior of $R(b)$ functions at this case and all discussed above reactions indicates a high degree of peripherality of the nucleon transfer processes (ΔR/R≤0.1) except for the reaction (d,p) – see below.

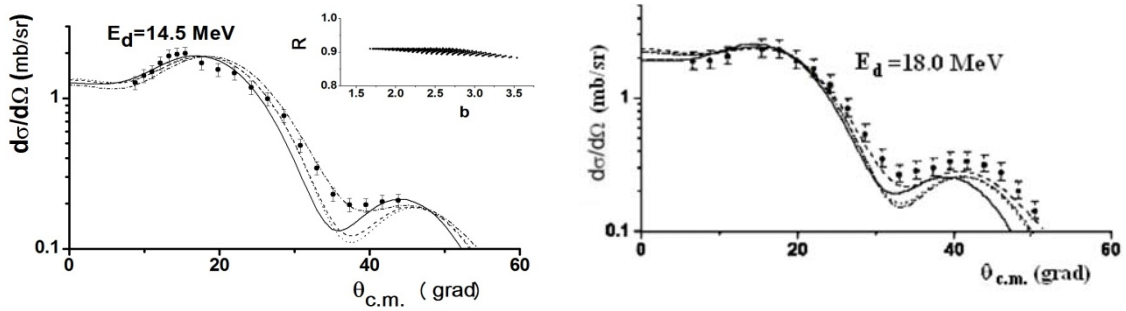

Fig. 2. Experimental and calculated DCSs of the reaction ^{25}Mg(d,t)^{24}Mg$_{g.s.}$. The curves are the DWBA calculations with the global OP and several sets of the optical parameters used in [15] and [6].

The experimental DCSs of the peripheral reaction ^{24}Mg(d,n)^{25}Al$_{g.s.}$ at the energies 7 and 9 MeV [1] were analyzed for obtaining the ANC $C^2_{25Al\to24Mg+p}$ with use of the mentioned above global OP and those presented in [1].

The values of the ANC squares recommended in our work on the basis of the totality of analyzed experimental data (after weighted averaging by values for the selected sets of OP and by different energies in the input channels of the reactions) for the ground states of the mirror nuclei ^{25}Mg and ^{25}Al are as follows:

$$C^2_{25\mathrm{Al}\to24\mathrm{Mg+p}} = 4.57 \pm 0.49 \text{ fm}^{-1},\ C^2_{25\mathrm{Mg}\to24\mathrm{Mg+n}} = 1.80 \pm 0.10 \text{ fm}^{-1}$$

The analysis of the experimental data on the reaction ^{24}Mg(d,p)^{25}Mg was done at the energies E_d=13.6 MeV [5] and 14.5 MeV [6]. The calculated angular distributions of protons are presented in **Fig. 3** together with the mentioned experimental data.

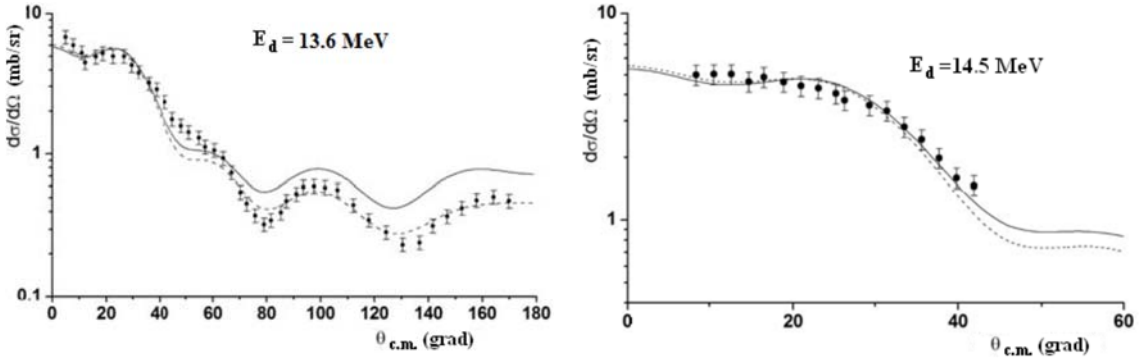

Fig. 3. Calculated and experimental angular distributions of protons from the reaction ^{24}Mg(d,p)^{25}Mg$_{g.s.}$ at E_d= 13.6 MeV [5] and 14.5 MeV obtained by us in [6].

Behavior of the function R(b) at both energies (see **Fig. 4**) indicates a strong non-peripherality of the neutron transfer in this reaction and, consequently, extraction of the ANC from the MDWBA analysis is incorrect. However, due to the defined value of the ANC from the analysis of the peripheral reaction ^{25}Mg(d,t)^{24}Mg, one can find the value of the spectroscopic factor (SF) *Z*. Moreover, the strong uncertainty of its value associated with ambiguity of the geometric parameters of the nuclear potential of the bound state ^{24}Mg+p is significantly minimized. Indeed, one can obtain the value $b=b_0$ by graphical solving the equation $R(b;[r_0,a])=R_{exp}$ (see **Fig. 4**), where R_{exp} is the constant, the uncertainty of which is determined only by the errors of the experimental DCS (see line in the figure and the error zone). The intersection point of the calculated function $R(b)$ with R_{exp} determines the value of a single-particle ANC $b=b_0$.

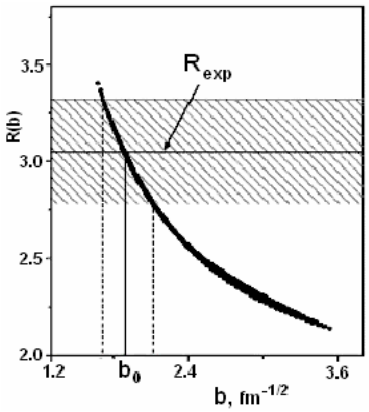

Fig. 4. Behavior of the function $R(b)$ for the reaction ^{24}Mg(d,p)^{25}Mg at the energy E_d=14.5 MeV.

Finally, we obtain the desired value of SF $Z_{25Mg\to24Mg+n} = Z_0 = C^2_{25Mg\to24Mg+n} / b_0^2$ from the well-known relation C^2=Zb^2 [16], $Z_{25Mg\to24Mg+n} = 0.41 \pm 0.13$.

References

[1] Bucciono S.G., et al. // Nucl. Phys. **86 (**1966) 353.
[2] Middleton R., Hinds S. // Nucl. Phys. **34 (**1962) 404.
[3] Gujes B. // Phys. Rev. **136** (1964) 1305.
[4] Hosono K. et al. // Journ. the Phys. Soc.Japan **25 (**1968) 36.
[5] Tokarevsky V.V., Shcherbin V.N. // Journ. Nucl. Phys (Rus). **22(**1975) 917.
[6] Artemov S.V., et al. // Reps of AS of Resp. Uzb. **3 (**2018) 38.
[7] Artemov S.V. et al. // Phys. At. Nucl. **71** (2008) 998.
[8] S.V. Artemov et al. Izv. NAS RK, ser. fiz-mat. **6** (2006) 61.
[9] H. An, C. Cai. // Phys. Rev. **C73** (2006) 9.
[10] Hinterberger F., et al. // Nucl. Phys. **A111** (1968) 265.
[11] Trost H.J., Lezoch P., Strohbusch U. // Nucl. Phys. A**462** (1987) 333.
[12] Perey C.M., Perey F.G. // Atomic data and nuclear data tables. **17** (1976) 1.
[13] Hamburger A.I. // Phys. Rev. **C118** №5 (1960) 1271.
[14] Gulamov I.R., et al. Abstr. 40th Ann. Conf. on Nucl. Spectrosc.& Struct. Atom. Nuclei – Leningrad, 1990. p.324.
[15] Artemov S.V. et al., // Uzb. Fiz. Journ. **11** №3 (2009) 166.
[16] Blokhintsev L.D. et al. // Fiz. Elem Particles&Atomic Nuclei (Moscow). **8 (**1977) 1189.

Role of the Dynamical Polarization Potential in Explaining the Low and Intermediate Energy Data of Alpha+^{12}C System

Y. Kucuk[1], A. Soylu[2] and L. C. Chamon[3]

[1]*Akdeniz University, Department of Physics, Antalya, Turkey*
[2] *Niğde Omer Halis Demir University, Department of Physics, Niğde, Turkey*
[3]*Depto. de Fisica Nuclear, Sao Paulo University, SP, Sao Paulo, Brazil*

^{4}He+^{12}C system is one of the most studied systems since it plays crucial role in stellar nucleosynthesis [1-5]. The elastic scattering cross section of this system has been measured at wide energy range and accumulated data have been analyzed in general by using Optical model. While the phenomenological potentials could explain the elastic scattering cross section data at high energies, they failed to produce the elastic scattering cross section at low and intermediate energies. Due to failure of the Woods-Saxon shaped optical potential, we attempted to analyze low and intermediate energy data in the framework of the double folding model. For the calculations at 13, 18, 29, 35, 41 54.1 and 60 MeV, we have used microscopic Sao-Paulo potential as well as the semi-microscopic optical potential which consists of standard folded real part and Woods-Saxon shaped imaginary part. However, we have observed that the folding potential does not provide a better agreement than the phenomenological potential in explaining the data at these energies. Recent studies have shown the coupling to the non-elastic channels has significant effect on the reaction observables of alpha induced interactions at low energies [6]. Therefore we have modified the shape of the real and imaginary potential simultaneously by adding two Woods-Saxon shaped potentials, given in Equation 1, at the surface region to include the dynamical polarization potential (DPP) which takes into account the coupling effects to the non-elastic channels. In this work we have shown DPP is very effective to produce the elastic scattering cross section data of alfa+^{12}C system at low and intermediate energies.

$$V_{DPP}(r) = \frac{-V_0}{1+e^{\frac{r-R_v}{a_v}}} + \frac{-W_0}{1+e^{\frac{r-R_w}{a_w}}} \qquad (1)$$

$R_v = r_v[A_p+A_T]$ and $R_w = r_w[A_p+A_T]$

The results of the analyses for the energies 13, 18, 54.1 and 60 MeV have been discussed in 12th International conference 'Nuclear and Radiation Physics' held in Almaty, Kazakhstan, 23-27 June 2019. These results have also been submitted to the Nuclear Physics A to publish. In this paper we present the results at energies 29, 35 and 41 MeV in **Fig. 1**. As seen from the figure DPP provides an improvement in explaining the data particularly at 29 MeV. At 35 and 41 MeV bare folding is also successful to describe the cross section data and DPP do not make significant contribution at these energies.

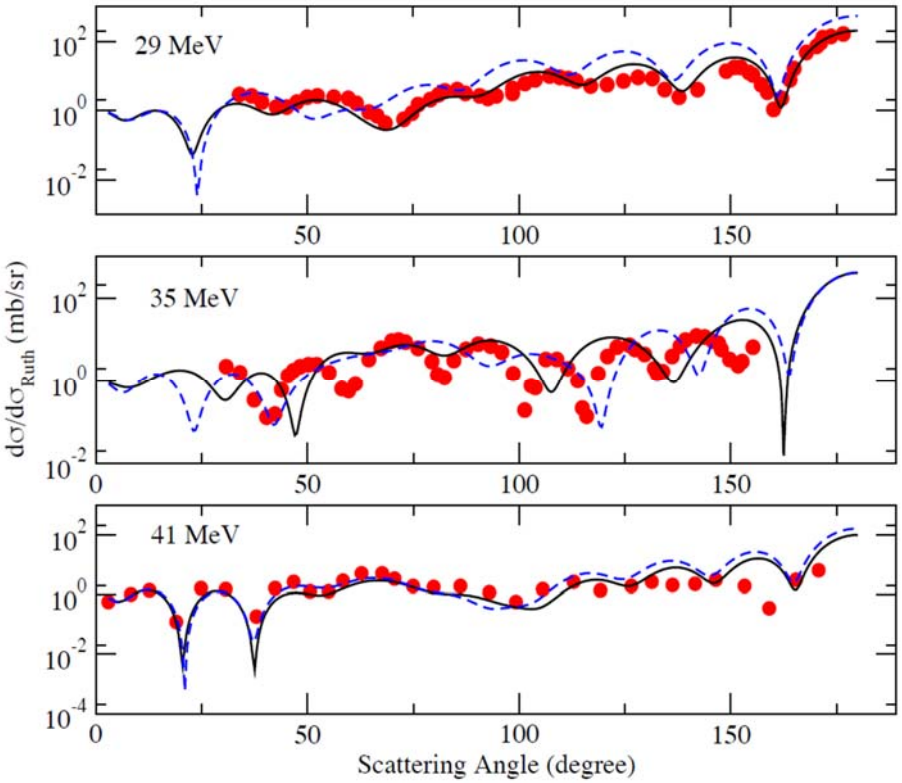

Fig. 1. Elastic Scattering Cross section data at 29, 35, 41 MeV. Here circles show the experimental data, dashed lines show the standard folding potential results and solid lines shows the folding potential + DPP effect.

We have also applied the same modified folding potential which includes DPP effect to obtain the energies of resonant states of ^{16}O by using Gamow code [7] (**Fig.2**). All results were obtained by fixing the excitation energy of the 4^+ state to constrains the potential. Experimental excitation energies and decay widths values are taken from Refs. [8] and [9]. We have used the following N_R values: 0.860 the potential at 29 MeV, 0.841 for DF potential at 35 MeV, 0.917 for DF+DPP potential at 41 MeV.

In summary, we have analyzed the elastic scattering data of the alfa+^{12}C system at some energies within the framework of the double folding model. We have also calculated alfa-cluster states in ^{16}O by using the same potential. We have shown that including of DPP in the bare folding potential improves the results in producing the elastic scattering cross section and also the rotational bands of ^{16}O.

Y. Kucuk acknowledges that this work was supported by Scientific Research Project Coordination Unit of Akdeniz University. Project number: 3518.

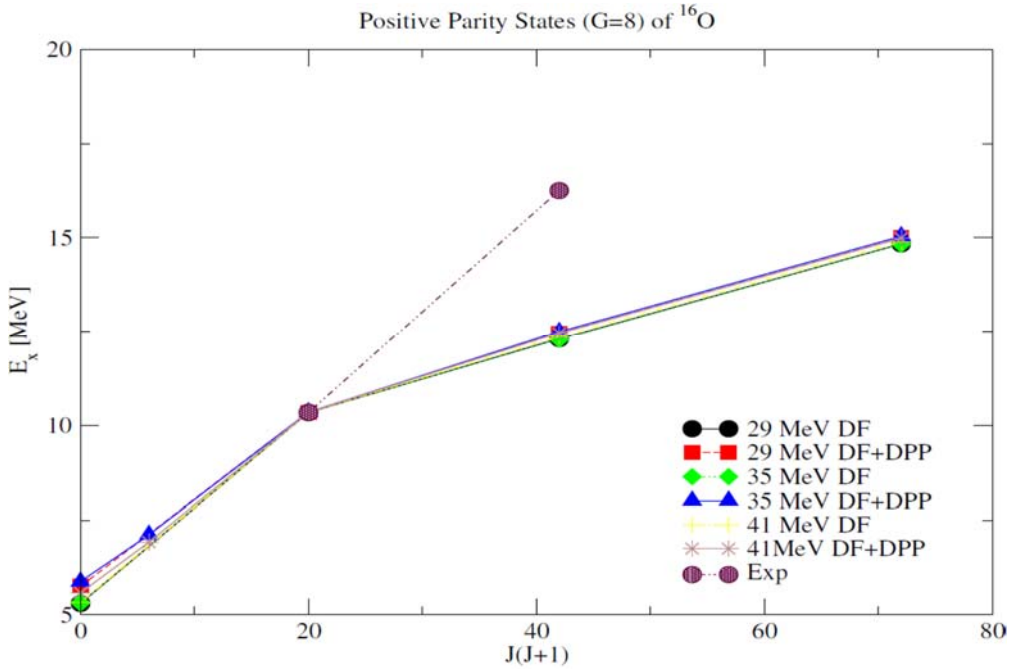

Fig. 2. Excitation energies for ^{16}O versus J(J + 1) for G=8, positive parity states for DF and DF+DPP potentials.

Table-1. The potential parameters of the Folding model calculations. N_r is the normalization constant of the real potential and W, r_w, a_w are the parameters of the Woods-Saxon shaped imaginary potential.

E_{LAB} (MeV)	N_r	W (MeV)	r_W (fm)	a_W (fm)
29.0	0.95	0.5	0.8	0.64
35.0	0.87	10.0	0.8	0.6
41.0	0.89	13.0	0.8	0.94

Table-2. The parameters of the Dynamical Polarization Potential, V shows the real part of DPP and W shows the imaginary part of DPP.

E_{LAB} (MeV)	V_0 (MeV)	r_v (fm)	a_v (fm)	W_0 (MeV)	r_w (fm)	a_w (fm)
29.0	8.0	0.7	0.75	2.0	0.8	0.94
35.0	-10.0	0.8	0.94	-1.0	0.8	0.94
41.0	5.0	0.7	0.6	1.0	0.8	0.94

References

[1] T. L. Belyaeva, A. N. Danilov, A. S. Demyanova, S. A. Goncharov, A. A. Ogloblin, and R. Perez-Torres Phys. Rev. **C82** (2010) 054618.
[2] S. A. E. Khallaf, A. M. A. Amry, and S. R. Mokhtar Phys. Rev. **C56** (1997) 2093.
[3] N. Baron, R. F. Leonard, and W. M. Stewart Phys. Rev. **C4** (1971) 1159.
[4] H. Oeschler, H. Fuchst, H. Schr¨oter, Nucl. Phys. **A202** (1973) 513-529.
[5] R. Lichtenthaler F., A. C. C. Villari, A. L´epine-Szily, and L. C. Gomes Phys. Rev. **C44** (1991) 1152.
[6] L. C. Chamon, L. R. Gasgues, L. F. M Alves, V. Guimaraes, P. Descouvemont, R. J. deBoer, and M. Weicher, Journal of Physics **G41** (2014) 035101.
[7] T. Vertse, K. F. Pal and Z. Balogh, Comp. Phys. Comm. **27** (1982) 309.
[8] F. Ajzenberg-Selove, Nuclear Phys. **A375** (1982) 1.
[9] L.L. Ames, Phys. Rev. **C25** (1982) 729.

Interaction of 30 MeV Energy Protons with Nuclei of Mass A=27-209

T.K. Zholdybayev

Institute of Nuclear Physics, 050032 Almaty, Kazakhstan

Working out the preequilibrium decay mechanism in nuclear reactions remains an actual problem of the nuclear reaction theory. The problem is largely connected with obtaining the new experimental data on double-differential cross sections in (*p*,*xp*), (*p*,*xd*), etc., reactions with different proton energies. These reactions play a role in the applied researches on secure and wasteless nuclear power system creation accelerator subcritical reactor. In this respect, there is a problem of determining the spatial and power distribution of the secondary particles, generated not only during the transition of the primary proton beam of target assembly and neutron flow, but also of more composite (^{2,3}H, ^{3,4}He) particles, which can represent themselves as initiators of the reactions by emitting neutrons.

Reviews on available experimental data of reactions with nucleons are presented in [1, 2]. Several experiments on double-differential cross sections measurements have been performed at energy about 30 MeV [3–7]. More over at this energy many channels of reactions are open, and the total cross section of the reactions for nuclei of such mass region reaches its maximum [8].

The experimental cross-section measurements of (*p,xp*) reaction were carried out on a beam of accelerated protons at the energy of 30 MeV on the isochronous cyclotron, U-150M, at the Institute of Nuclear Physics by using a self-supporting targets of ^{27}Al, ^{120}Sn, and ^{207}Pb which have been chosen as the objects of our investigation since they are the construction elements of a hybrid nuclear energy plant and experimental data on which are necessary for the development of ADS systems [9].

The systematic uncertainties were conditioned by the uncertainties in determining the target thickness (7%), the calibration of the current integrator (1%), and the solid angle of the spectrometer (1.3%). The energy of the accelerated particles was measured accurately within 1.2%. The whole systematic error was less than 10%. The experimental integral spectra were obtained after integrating the double-differential cross-sections on angle (**Fig. 1-3**).

Many different theoretical approaches have been used to describe the preequilibrium reaction data over a wide range of incident energies. In this work, the analysis of the experimental results has been conducted in the Griffin exciton model of the preequilibrium decay of nuclei. The program PRECO-2006, which describes the emission of particles with mass numbers from 1 to 4, has been used in our theoretical calculations. The Griffin exciton model is a statistical model, which describes the excited levels of the intermediate system in terms of the single-particle shell model, i.e.,

characterized by the number of the excited particles (above the Fermi level) and holes (below the Fermi level). From comparison of experimental and calculated integral spectra it is follows that main contribution in hard part of total cross section is due to exiton mechanism.

The analysis of the experimental results of reactions (p,xp) at E_p = 30.0 MeV was performed in the framework of the exciton model of nuclear decay [10] describing the transition of the excited system to the equilibrium state. In the two-component exciton model, proton and neutron degrees of freedom are taken into account separately [11] and it is assumed that the nucleus is characterized by the parameters p_π, h_π, p_ν and h_ν, where p and h denote particle and hole, and π and ν are proton and neutron degrees of freedom, respectively. The compound nucleus is formed with a particle-hole configuration that takes into account only the incident nucleons as particle degrees of freedom and does not take into account the hole ones. This configuration is denoted as (p_π, h_π, p_ν, h_ν) = (Z_a, 0, N_a, 0), where a refers to the bombarding particle. The difference between the number of particles and holes during the transition to the equilibrium state is constant. Calculations of the one-particle states density are calculated separately for protons $g_{\pi 0}$ and neutrons $g_{\nu 0}$:

$$g_{\pi 0} = \frac{Z}{K_g}, \quad g_{\pi 0} = \frac{Z}{K_g}, \tag{1}$$

$$g_{\nu 0} = \frac{N}{K_g}, \quad g_{\nu 0} = \frac{N}{K_g}, \tag{2}$$

where K_g is normalization factor. Particle-hole states density [12] is given by:

$$\begin{aligned} \omega_{ESM}(p, p_\pi, E) &= \frac{\left(g_{\pi 0}\right)^{n_\pi} \left(g_{\nu 0}\right)^{n_\nu} (E - A(p, p_\pi, E))^{n-1}}{p_\pi! h_\pi! p_\nu! h_\nu (n-1)!}, \\ \omega_{ESM}(p, p_\pi, E) &= \frac{\left(g_{\pi 0}\right)^{n_\pi} \left(g_{\nu 0}\right)^{n_\nu} (E - A(p, p_\pi, E))^{n-1}}{p_\pi! h_\pi! p_\nu! h_\nu (n-1)!}, \end{aligned} \tag{3}$$

where $A(p,p_\pi,E)$ is the correction factor for the Pauli exclusion principle. These densities are used to calculate the probabilities of transitions that shift the nucleus from one particle-hole configuration to another.

Assuming that residual two-particle interactions are weak, we use the first-order perturbation theory to find the probability of intranuclear transitions (per unit time) λ [13]:

$$\lambda = (2\pi/\hbar)\left\langle |M|^2 \right\rangle \omega, \quad \lambda = (2\pi/\hbar)\left\langle |M|^2 \right\rangle \omega, \tag{4}$$

where $|M|^2$ is the rms matrix element of the intensity of intranuclear transitions (i.e., transitions between states with different n), and ω is the density of the final states that can realistically be achieved upon a given transition. It is assumed that the matrix elements have the same form and differ by only normalization factor [8]:

$$\begin{aligned} \left|M_{ij}\right|^2 &= K_{ij} A_a g_0^{-3} \left(\frac{E}{3A_a} + 20.9\right)^{-3}, \\ \left|M_{ij}\right|^2 &= K_{ij} A_a g_0^{-3} \left(\frac{E}{3A_a} + 20.9\right)^{-3}, \end{aligned} \tag{5}$$

where A_a is the mass of an incident particle.

At any stage of system relaxation, the emission of type b particles into the channel with energy ε is possible. The rate of particle emission from this state is calculated using the formula

$$W_b(p, p_\pi, E, \varepsilon) = \frac{2s_b + 1}{\pi^2 \hbar^3} \mu_b \varepsilon \sigma_b(\varepsilon) \frac{\omega(p_\pi - Z_b, h_\pi, p_\nu - N_b, h_\nu, U)}{\omega(p_\pi, h_\pi, p_\nu, h_\nu, E)}, \tag{6}$$

where Z_b and N_b are the numbers of protons and neutrons of the emitted particle, s_b is the particle's spin, and μ_b is its mass; $\sigma_b(\varepsilon)$ is the cross section of the inverse process of the formation of a compound nucleus; and U is the excitation energy, defined as $U = E - \varepsilon - B_b$ where B_b is the bonding energy of the emitted particle.

Theoretical calculations were performed using the PRECO–2006 code [14] optimized for the case under consideration. We chose the $(p_\pi, h_\pi, p_\nu, h_\nu) = (1,0,0,0)$ particle–hole configuration as our starting point. The normalization coefficient K_g was taken to be 15 MeV. The square of the matrix elements was parameterized using the normalization constants $K_{\pi\pi}$: $K_{\pi\nu}$: $K_{\nu\nu}$= *2200:900:900 МэВ*^{2}.

Fig. 1 to 3 show the theoretical and experimental data on the double differential and integral cross-sections for (p,xp) reactions on the ^{27}Al, ^{120}Sn, and ^{207}Pb nuclei. It follows from a comparison of the experimental and theoretically calculated integral spectra that the main contribution to the formation of the integral cross section for (p,xp) reactions comes from the preequilibrium mechanism.

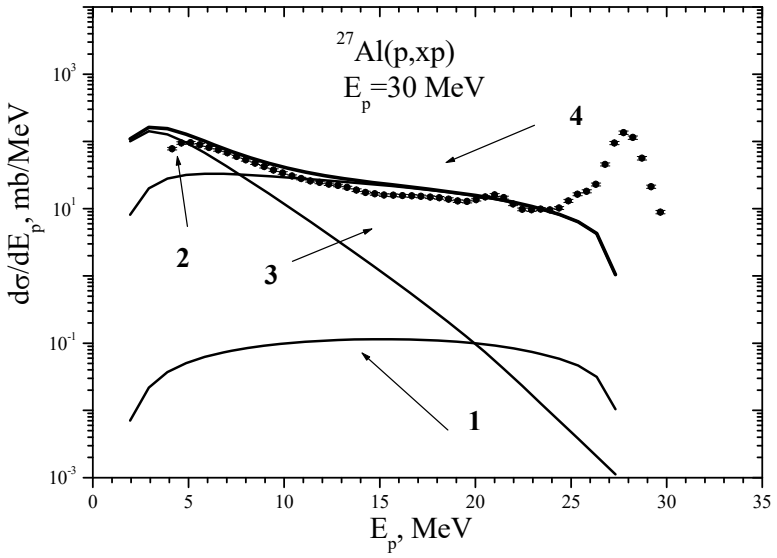

Fig. 1. Comparison of the experimental integrated cross sections for ^{27}Al(p,xp) reactions with calculations within the exciton model. Symbols show the experimental values. (1) single-stage processes, (2) emission of particles from the equilibrium state, (3) pre-equilibrium component, (4) total integral cross section.

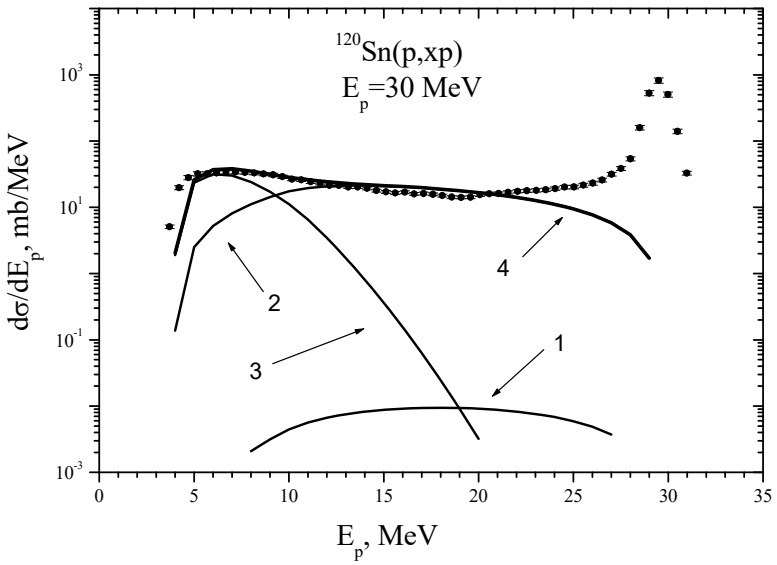

Fig. 2. Comparison of the experimental integrated cross sections for ^{120}Sn(p,xp) reactions with calculations within the exciton model. Symbols show the experimental values. (1) single-stage processes, (2) pre-equilibrium component, (3) emission of particles from the equilibrium state, (4) total integral cross section.

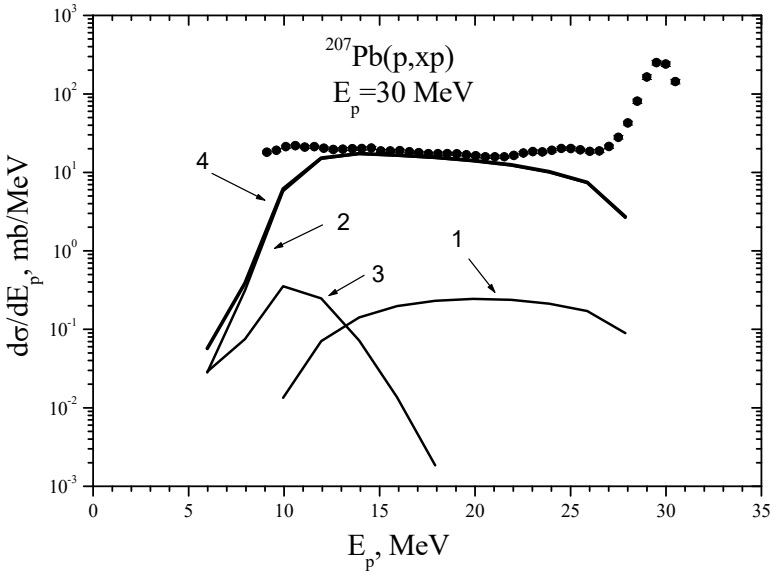

Fig. 3. Comparison of the experimental integrated cross sections for 207Pb(p,xp) reactions with calculations within the exciton model. Symbols show the experimental values. (1) single-stage processes, (2) pre-equilibrium component, (3) emission of particles from the equilibrium state, (4) total integral cross section.

This experimental study is very important for the extension of the preequilibrium experiments in this direction to see the mechanism of the reaction and the level of energy dependence. It is also important to observe the adequacy of the above-mentioned theoretical models to explain the measured experimental data.

This work was supported by the Program #BR05236494 «Fundamental and applied studies in related fields of physics of terrestrial, near-earth and atmospheric processes and their practical application».

References

[1] P.E. Hodgson, E. Betak, Phys. Rep. **374** (2003) 1.
[2] A.J. Koning, M.C. Duijvestijn, Nucl. Phys. **A744** (2004) 15.
[3] F.E. Bertrand and R.W. Peelle, Phys. Rev. **C8** (1973) 1045.
[4] Y. Watanabe et al., Phys. Rev. **C51** (1995) 1891.
[5] A. Duisebayev, K.M. Ismailov, I. Bostosun, Phys. Rev. **C67** (2003) 044608.
[6] A. Duisebayev, K.M. Ismailov, I. Bostosun, Phys. Rev. **C72** (2005) 054604.
[7] A. Duisebayev et al., Bull. of RAS. Physics. **78** (2014) 601.
[8] J.J. H. Menet, et al., Phys. Rev. **C4** (1971) 1114.
[9] Y. Ikeda, Journal of Nuclear Science and Technology **Suppl.2** (2002) 13.

[10] J.J. Griffin, Phys. Rev. Lett. **№9** (1966) 478.
[11] C. Kalbach, Phys. Rev. **C33** (1986) 818.
[12] .F.C. Williams, Nucl. Phys. **A166** (1971) 231.
[13] F.C. Williams, Phys. Lett. **B31** (1970) 184.
[14] Kalbach C. PRECO-2006: Exiton model preequilibrium nuclear reaction code with direct reaction. Durham NC 27708-0308, 2007

Overview of EXFOR Compilation Activity in Mongolia between 2018 and 2019

M. Odsuren[1,2] and N. Otuka[3]

[1]*School of Engineering and Applied Sciences, National University of Mongolia, Mongolia*
[2] *Nuclear Research Center, National University of Mongolia, Mongolia*
[3]*Nuclear Data Section, IAEA, Vienna, Austria*

The Nuclear Research Center (NRC), National University of Mongolia–International Atomic Energy Agency (IAEA) collaboration was built in 2014 for compilation of heavy-ion (A>12) induced reaction data measured in West European countries for the EXFOR library [1]. The NRC is the first nuclear research and educational institution in Mongolia, which carries out basic and applied research of low energy nuclear physics.

In the four years since the launch of the NRC-IAEA collaboration (2014-2017), 35 articles published between 2002and 2017 [2] were compiled and uploaded into the EXFOR database.

For the recent two years (2018-2019), wecomplied17 EXFOR entries from articles published between 2005 and 2019 (**Table 1**). Seven of them compile heavy-ion induced reaction data measured at Italian laboratories and the others compile heavy-ion induced reaction data measured at the GANIL (France), GSI(Germany), University of Jyväskylä (Finland), Australian National University (Australia) and Nuclear research center (Mongolia). The last article is not for heavy-ion induced reaction data, but it was compiled to satisfy the needs of experimental data for update of evaluated fission product yields [3].

So far we have received numerical data for all cases, and it enables us to avoid compilation of digitized data.

References

[1] N. Otuka et al., "Towards a More Complete and Accurate Experimental Nuclear Reaction Data Library (EXFOR): International Collaboration Between Nuclear Reaction Data Centres (NRDC)", Nucl. Data Sheets **120** (2014) 272.
[2] M. Odsuren, N. Otuka, INDC(JP)-0200, International Atomic Energy Agency (2016) 57; INDC(MNG)-0001, International Atomic Energy Agency (2018) 40.
[3] O. Schwerer, B. Pritychenko, “Completeness check EXFOR vs. NSR: Photofission yields”, Memo CP-C/465, National Nuclear Data Center (2019).

Table 1. List of compiled articles.

Entry	First author	Journal volume, page and publication year+	Laboratory, country	Year+	Status*
D0851	M.J.Ermamatov	J,PR/C,96,044603,2017	LNL, INFN, Italy	2018	in EXFOR
D0883	S.Lukyanov	J,JP/G,37,105111,2010		2018	in EXFOR
D0894	B.Paes	J,PR/C,96,044612,2017	LNS, INFN, Italy	2018	in EXFOR
D0899	G.Montagnoli	J,PR/C,97,024610,2018	Padova, INFN, Italy	2018	in EXFOR
D0904	G.Colucci	J,PR/C,97,044613,2018	Padova, INFN, Italy	2018	in EXFOR
D0905	V.A.B.Zagatto	J,PR/C,97,054608,2018		2018	in EXFOR
D0908	D.Pereira	J,PL/B,710,426,2012	LNS, INFN, Italy	2018	in EXFOR
D0909	N.D.Trinh	J,NIM/A,896,152,2018	GANIL, France	2018	in EXFOR
D0918	E.N.Cardozo	J,PR/C,97,064611,2018	LNS, INFN, Italy	2018	in EXFOR
D0919	F.Wamers	J,PR/C,97,034612,2018		2018	in EXFOR
D0920	R.Linares	J,PR/C,98,054615,2018	LNS, INFN, Italy	2018	in EXFOR
D0923	R.Briselet	J,PR/C,99,024614,2019	University of Jyväskylä, Finland	2019	in EXFOR
D0931	B.Fernandez-Dominguez	J,PL/B,779,124,2018	GANIL, France	2019	in EXFOR
D0932	E.Prasad	J,PR/C,96,034608,2017	Australian National University, Australia	2019	in EXFOR
D0935	I.Stefan	J,PL/B,779,456,2018	GANIL, France	2019	in EXFOR
D0941	S.Bagchi	J,PL/B,790,251,2019	GSI, Darmstadt, Germany	2019	in EXFOR
G0065	N.Norov	C,ISSP-III,30,2005	Nuclear Research Center, Mongolia	2019	PRELIM

+PR/C: Phys. Rev. C, JP/G: Journal of Physics G, PL/B: Phys. Lett. B, NIM/A: Nuclear Instruments and Methods A, C,ISSP-III: Conference proceedings

* "in EXFOR": The EXFOR entry is accessible through the EXFOR web retrieval systems."PRELIM": The EXFOR entry was created and under review by other centres.
+ Year = Year of compilation.

Analyzing the (p, xp) and (p, xα) Reactions on ^{59}Co at E=30 MeV by Using the Statistical Models

K. Azhdarli[1], Y. Kucuk[1], B. Canbula[2], T. Zholdybayev[3,4], Zh. Mukan[3,5], B. Emre[1], E.B. Sapmaz[1], I. Boztosun[1]

[1] *Akdeniz University, Antalya, Turkey*
[2] *Manisa Celal Bayar University, Manisa, Turkey*
[3] *Institute of Nuclear Physics, Almaty, Kazakhstan*
[4] *Al Farabi Kazakh National University, Almaty, Kazakhstan*
[5] *Gumilev Eurasian National University, Nur-Sultan, Kazakhstan*

Investigation of the astrophysical rp and p-processes which occur in the stars is one of the most interested subjects in the field of nuclear physics and nuclear astrophysics. Pre-equilibrium reactions play key role during nucleosynthesis in Early Universe and thus it has been studying extensively [1]. The dynamics of the transition from the excited nuclear states to the equilibrium still wait to be understood [2-5]. Therefore, new experiments must be conducted at different energy ranges and accumulated high quality data must be analysed in detail. In this work, we aim to provide a new experimental data and to explore the various interaction effects on the (p,xp) and (p,xα) reactions. We present a new measurement of (p,xp) and (p,xα) differential cross section on cobalt (^{59}Co) at E_{Lab}=30 MeV and the first theoretical analysis of these experimental data in the framework of the statistical models.

The experimental complex is located on the isochronous cyclotron U-150M of the Institute of Nuclear Physics, Kazakhstan. Measuring-computing complex was adapted for the measurement of the inclusive spectra of protons and alpha-particles in the maximum possible energy range of the secondary particles. The measurements of cross-sections of nuclear reaction products were carried out using a scattering chamber, equipped with a rotary spectrometer of charged particles, monitor of the scintillation detector, installed at an angle of 30^0, target drive systems, collimation system and the Faraday cylinder to measure the number of particles passing through the target.

For the compound nucleus calculations, we have used Hauser-Feshbach Model which is one of the most successful statistical models. This model takes into account of different J and π states for formation compound nucleus. Hauser–Feshbach equation is given by,

$$\sigma_{cc'} = \frac{\pi}{k^2}\sum_j \frac{(2j+1)}{(2i_c+1)(2I_c+1)} \frac{\sum_{s,l} T_s(c) \sum_{s',l'} T_{s'}(c')}{\sum_c \sum_{s,l} T_l(c)} \quad (1)$$

Cross sections have been calculated by TALYS 1.9 nuclear reaction code [6]. The global parameterization of Koning and Delaroche [7] for the optical model potential for protons is used as a starting point to determine local parameters. For the real component

of the volume-central potential we have used an existing proton elastic scattering data on Co-59 of Ridley [8] at 30 MeV, and we have obtained values:

$$V_V = 55.86MeV, r_V = 1.080fm, a_v = 0.816fm. \quad (2)$$

With these real potential we achieved a very good agreement with the experimental data, which is given in **Fig. 1**. Once we adjusted the volume-central potential parameters to the elastic scattering data, we have used the surface potential to reproduce (p,xp) data. The global parameterization of Koning and Delaroche [7] suggests $r_D = 1.281fm$ and $a_D = 0.549fm$ for the geometry of the both real and imaginary components of the surface potential and we have used these values with the adjusted potential depths:

$$V_D = 4MeV, W_D = 2MeV. \quad (3)$$

For pre-equilibrium calculations, we have used multi-step direct/compound model with a scale factor 0.6 and with this parameter set we have a very satisfying explanation of the experimental data of (p,xp) reaction, which is given in **Fig. 1**.

For (p,xα) reaction we have used the same parameterization as described above for the incident channel and we have tried to reproduce the (p,xα) data by adjusting the parameters for the exit channel. For the optical model potential for alpha on Fe-56 we have used the global parameterization of Avrigeanu [9], which is the default option in TALYS. We adjusted the real component of the volume-central potential by reducing the both depth and geometry parameters with a 0.8 factor. The comparison between the estimated cross sections with the experimental data is given in **Fig. 2**.

With the optical model potential parameter set described above we attempted to reproduce the cross sections of both Co-59(p,xp) and Co-59(p,xα) reactions. The agreement with the experimental data could be improved by using microscopic potentials rather than a phenomenological potential for the optical model calculations.

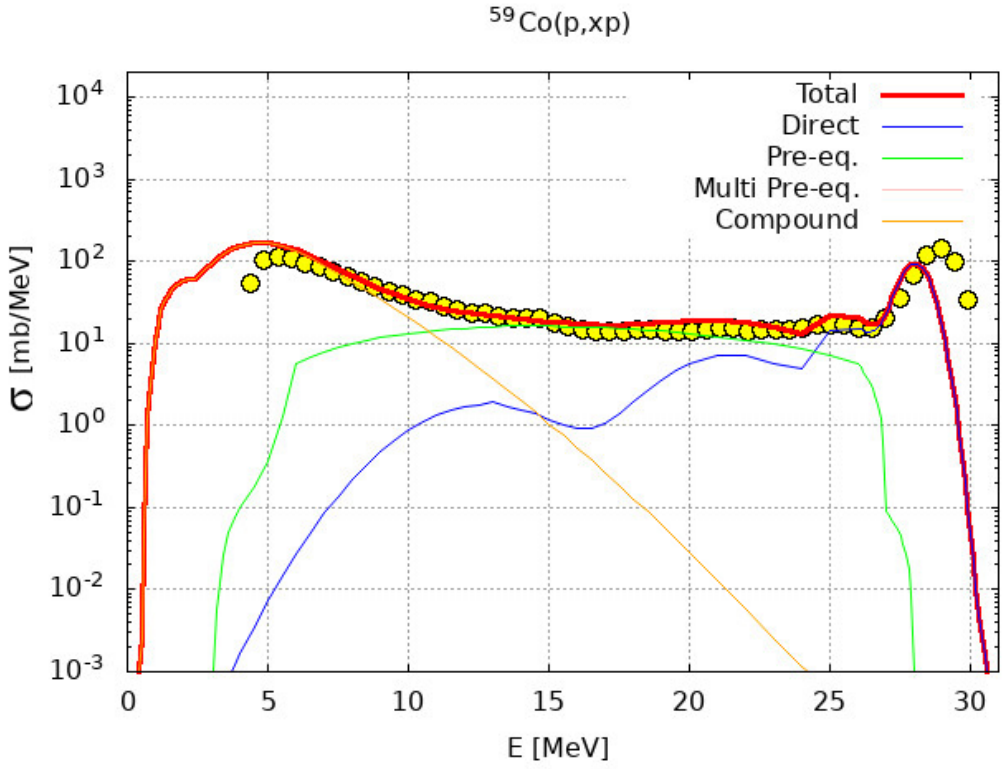

Fig. 1. The analysis of the total cross section for the (p, xp) reaction.

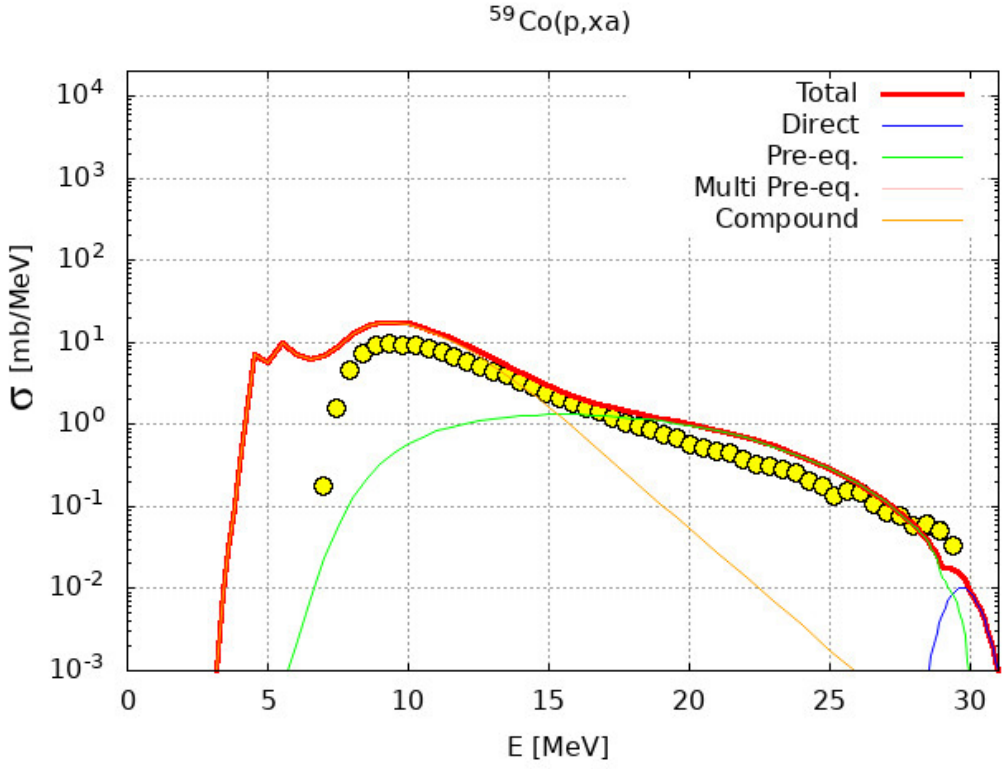

Fig. 2. The analysis of the total cross section for the (p, xα) reaction.

This work has been supported by Scientific and Technical Research Council of Turkey, (TUBITAK). Project number is 118R029. Y. Kucuk thanks TUBITAK and Kazakhstan Nuclear Physics Institute.

References

[1] K. Langanke and M. Wiescher, Rep. Prog. Phys. **64** (2001) 1657.
[2] G. M. Gurevich,, L.E. Lazareva, V. M. Mazur, S. Merkulov, G.V. Solodukhov and V. Tyutin,, Nucl. Phys. **A351** (1981) 257.
[3] Y. Watanabe, A. Aoto, H. Kashimoto, S. Chiba, T. Fukahori, K. Hasegawa, M. Mizumoto, S. Meigo, M. Sugimoto, Y. Yamanouti, N. Koori, M. B. Chadwick and P. Hodgson,, Phys. Rev. **C51** (1995) 1891.
[4] Y. Watanabe, K. Kodaka, Y. Kubo, N. Koori, M. Eriguchi and M. Hanada. Z Physics. **A336** (1990) 63.
[5] A. Duysebaev, K.M. Ismailov and I. Bostosun, Physical Review. **C67** N4 (2003) 044608.
[6] A.J. Koning, S. Hilaire, M.C. Duijvestijn, "TALYS-1.0", Proceedings of the International Conference on Nuclear Data for Science and Technology, April 22-27, , Nice, France, editors O. Bersillon, F. Gunsing, E. Bauge, R. Jacqmin, and S. Leray, EDP Sciences, (2007) 211.
[7] A.J. Koning, J.P. Delaroche, Nucl. Phys. **A713** (2003) 231.
[8] B.W. Ridley, J.F. Turner, Nucl. Phys. **58** (1964) 497.
[9] V. Avrigeanu et al. Phys. Rev. **C90** (2014) 044612.

Experimental Studies of Cosmic Rays at the Laboratory of Cosmic Rays Variations of Al-Farabi Kazakh National University

N.O. Saduyev [1,2,3], O.A. Kalikulov [1,2,3], A.L Shepetov [4], Y.S. Mukhamejanov [1,2,3,5], N.O. Yerezhep [1,2], S.K. Shinbulatov [1,2], A.I. Zhumabayev [1,2], Sh.B. Utey [1,2], A.E. Baktoraz [1,2]

[1]*Al-Farabi Kazakh National University, Almaty, Kazakhstan*
[2]*National Nanotechnology Laboratory of Open Type, Almaty, Kazakhstan*
[3]*Institute of Experimental and Theoretical Physics, Almaty, Kazakhstan*
[4]*P.N. Lebedev Physical Institute of the Russian Academy of Sciences, Moscow, Russia*
[5]*Institute of Nuclear Physics, Almaty, Kazakhstan*

Introduction - About the laboratory

The Laboratory of Cosmic Rays Variations (LCRV) neutron monitors are located in Almaty at al-Farabi Kazakh National University (KazNU) campus (897 m above sea level). Today there are several experiments are running at the Laboratory allowing register different types of cosmic rays components as well as Extended Air Showers (EAS).

Scientific areas of LCRV are

1. Physics of high and ultra-high energies.
2. Nuclear astrophysics.
3. Nuclear electronics.

The laboratory of cosmic ray variations is currently developing new directions that are included in international programs:

1. Monitoring of cosmic rays by terrestrial and stratospheric methods;
2. Solar-terrestrial relations;
3. Near-Earth space.

The laboratory history starts in 1957 with the start of operation of IGY-57 neutron monitor. Today the following setups are being run by the laboratory: IGY-57 neutron monitor (**Fig. 1**), neutron supermonitor 6NM-64 (since 1980s) and a narrow-body muon telescope with a total area of 6 m^2. The data obtained are used to conduct research in KazNU, scientific institutions of Kazakhstan and other countries, as well as in the form of daily reports sent to the European database of neutron monitors, which, in accordance with international treaties, sends them around the world in the public domain.

Several programs are carried out under the auspices of the "International Union of Pure and Applied Physics", with the participation of scientists from Russia, USA, etc. Work is also underway to create a software and hardware complex for collecting data for scientific experiments.

Fig. 1. Neutron monitors 6NM-64 (top) and IGY-57 (bottom).

Research objectives of Narrow Body Muon Telescope: Registration of flare phenomena on the Sun and the processes of transfer of magnetized plasma into near-Earth space using a muon telescope to study the development of these physical phenomena over time and, in particular, to study the mechanisms of the influence of solar activity on the earth's atmosphere;

Real time monitoring of changes in the characteristics of the atmosphere (temperature, air density) using a muon telescope for scientific research of atmospheric physics;

Development of a new registration system with online recording to the database.

At present, the Laboratory of Cosmic Rays Variation is working on the creation of experimental facilities based on ionization chambers and scintillation detectors to study extended air showers (EAS) generated by high-energy and ultra-high-energy cosmic rays. In particular, an installation is being developed for measuring the sizes of EAS cores, which allows the restoration of the mass composition of the primary cosmic rays.

A meeting with CERN scientists representing the CMS and ATLAS collaborations is scheduled for this August. During the meeting, prospects for signing a protocol on scientific and technical cooperation in the CMS and ATLAS collaborations and the possibility of obtaining the status of a permanent member of the collaboration will be discussed.

2 Database

2.1 European database

Two neutron monitors 6NM-64 and IGY-57 are operating for measurements of the intensity of the hadron component of high-energy cosmic rays (>10^9 eV). The data acquired by the monitors can be accessed remotely from website [1]. The 6NM-64 neutron monitor is also a part of Real-Time Database for high-resolution Neutron Monitor measurements (**Fig. 2**), which provides access to Neutron Monitor measurements from stations around the world. The goal of NMDB is to provide easy access to all Neutron Monitor measurements through an easy to use interface. NMDB provides access to real-time as well as historical data. These data are free for non-commercial use within the restrictions imposed by the providers. If you use such data for your research or applications, please acknowledge the origin by a sentence like "We acknowledge the NMDB database (www.nmdb.eu), founded under the European Union's FP7 programme (contract no. 213007) for providing data.", and acknowledge individual monitors following the information given on the respective station information page (see sub-pages under www.nmdb.eu). [2].

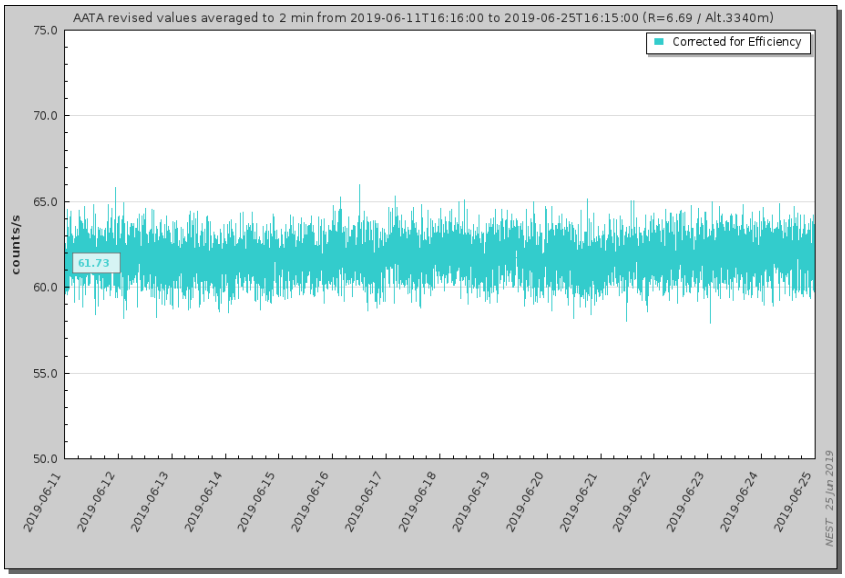

Fig. 2. Data plot taken by NMDB tools from our 6NM64 neutron monitor for the last 14 days.

2.2 KazNU database

The data acquired by the IGY-57 and 6NM-64 neutron monitors can be accessed live at KazNU neutron monitors database website (**Fig 3, 4**) [3]. Observation data allow us to study the known types of cosmic ray variations with good accuracy, to detect the fine structure in changes in cosmic ray intensity (the so-called microvariations of cosmic rays)

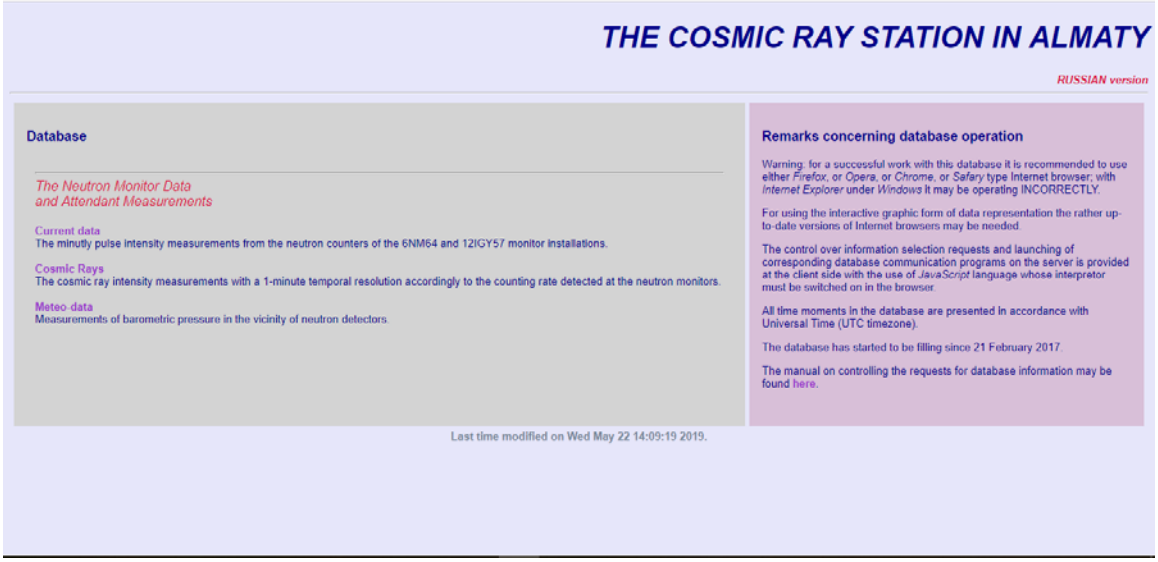

Fig. 3. The main page of the website of the database.

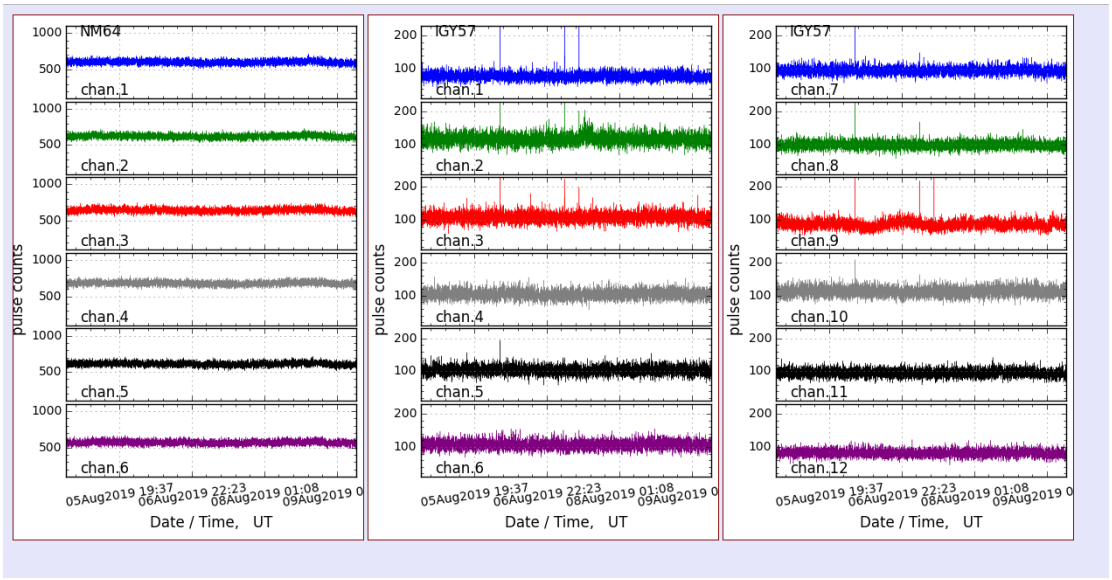

Fig. 4. The minutely pulse intensity measurements from the neutron counters of the 6NM64 and 12IGY57 monitor installations.

2.3 CANRDB database

Also, there is an active collaboration with a Central Asia Nuclear Reaction Database, to create section for cosmic rays database (**Fig. 5**). Central Asian Nuclear Reactions Data Base (CANRDB) was founded in April 2012. The foundation of CANRDB was supported by the Japanese Charged Particle Reaction Group (Hokkaido University, Japan), Centre For Photonuclear Experiments Data (Lomonosov MSU,

Russia) and International Atomic Energy Agency (IAEA). CANRDB is a member of International Network of Nuclear Reaction Data Centres (NRDC) under the auspices of IAEA.[4]

Fig. 5. The main page of the website of the database on cosmic rays and nuclear reactions.

2.4 The Tien-Shan Mountain Station's database

Tien-Shan Mountain Station has its own database website (**Fig. 6**) [5]. The database contains data on intensity measurements of the global cosmic ray flux and of local radiation background, The "THUNDERSTORM" Experiment: Electrons & Gammas, Extensive Air Showers, Weather, Applied Geophysics. The data is available in various formats such as: "Static plot", "Highcharts plot", "D3 plot", etc.

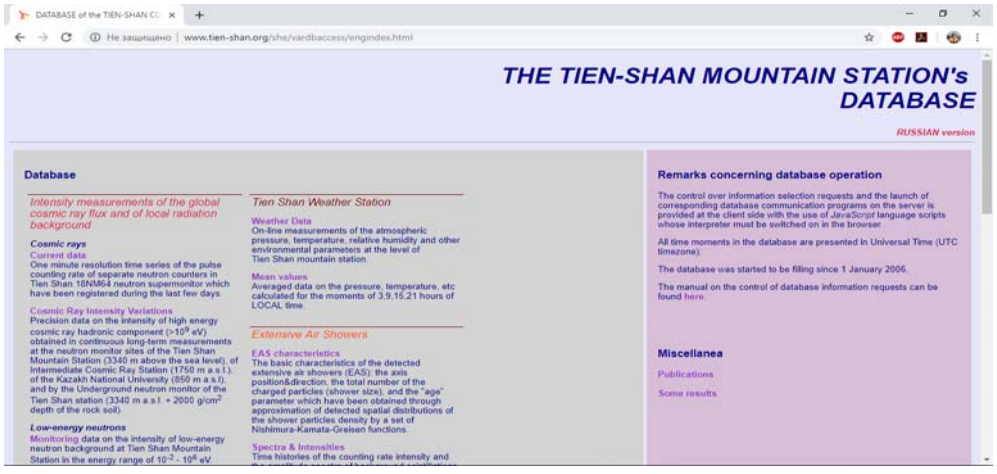

Fig. 6. The main page of the website of the database.

3 Acknowledgments

This work was supported by the Program #BR05236494 «Fundamental and applied studies in related fields of physics of terrestrial, near-earth and atmospheric processes and their practical application».

References

[1] http://www.tien-shan.org/she/vardbaccess/title.html
[2] http://www01.nmdb.eu/
[3] http://88.204.150.242/vardbaccess/
[4] http://canrdb.kaznu.kz/
[5] http://www.tien-shan.org/she/v http://www.tien-shan.org/she/vardbaccess/engindex.html ardbaccess/engindex.html

List of Participants

No.	Name	Affiliation	E-mail
1	Naohiko Otsuka	IAEA, Vienna, Austria	N.Otsuka@iaea.org
2	Timur Zholdybayev	INP, Almaty, Kazakhstan	zholdybayev@inp.kz
3	Myagmarjav Odsuren	NUM, Ulaanbaatar, Mongolia	odsuren@seas.num.edu.mn
4	Vidya Devi	IET, Bhaddal, India	vidyathakur@yahoo.co.in
5	Feruzjon Ergashev	INP, Tashkent, Uzbekistan	ergashev@inp.uz
6	Tetsuaki Tada	Department of Physics, Hokkaido University, Sapporo, Japan	tada@nucl.sci.hokudai.ac.jp
7	Sergey Artemov	INP, Tashkent, Uzbekistan	artemov@inp.uz
8	Yasemin Kucuk	Akdeniz University, Antalya, TURKEY	ykucuk@akdeniz.edu.tr
9	Y. S. Mukhamejanov	INP, Almaty, Kazakhstan	y.mukhamejanov@gmail.com
10	Nassurlla Burtebayev	INP, Almaty, Kazakhstan	burteb@inp.kz
11	B. M. Sadykov	INP, Almaty, Kazakhstan	sadykovbm@inp.kz
12	G. Ergaliev	Gumilev Eurasian National Univ., Nur Sultan, Kazakhstan	gani_ergaliuly@mail.ru
13	D. Alimov	INP, Almaty, Kazakhstan	diliyo@mail.ru
14	Zh. Kerimkulov	INP, Almaty, Kazakhstan	zhambul-k@yandex.ru
15	G. Ussabayeva	al Farabi Kazakh National University, Almaty, Kazakhstan	gulnazim1985@gmail.com

16	A. Pan	al Farabi Kazakh National University, Almaty, Kazakhstan	sofvillain1993@gmail.com
17	G. Alieva	Gumilev Eurasian National Univ., Nur Sultan, Kazakhstan	guli_alieva@mail.ru
18	Zh. Mukan	Gumilev Eurasian National Univ., Nur Sultan, Kazakhstan	zhuldiz_mukan@mail.ru
19	N. Yerezhep	al Farabi Kazakh National University, Almaty, Kazakhstan	nurzhan.yerezhep@gmail.com
20	T.N. Kvochkina	INP, Almaty, Kazakhstan	kvochtn@mail.ru
21	M. Nassurlla	INP, Almaty, Kazakhstan	nespad@mail.ru

Nuclear Data Section
International Atomic Energy Agency
P.O. Box 100
A-1400 Vienna
Austria

E-mail: nds.contact-point@iaea.org
Fax: (43-1) 26007
Telephone: (43-1) 2600 21725
Web: http://www-nds.iaea.org/